SYNTHESIS AND STRUCTURE OF N-HETEROCYCLIC CARBENE GOLD SULFIDE COMPLEXES

A Dissertation
Presented to
The Academic Faculty

by

Christopher Masanao Sato

In Partial Fulfillment
of the Requirements for the Degree
Master of Science in the
School of Chemistry and Biochemistry

Georgia Institute of Technology
May 2018

SYNTHESIS AND STRUCTURE OF N-HETEROCYCLIC CARBENE GOLD SULFIDE COMPLEXES

Approved by:

Dr. Joseph P. Sadighi, Advisor
School of Chemistry and Biochemistry
Georgia Institute of Technology

Dr. Jake D. Soper
School of Chemistry and Biochemistry
Georgia Institute of Technology

Dr. Henry S. La Pierre
School of Chemistry and Biochemistry
Georgia Institute of Technology

Date Approved: January 12, 2018

TABLE OF CONTENTS

LIST OF TABLES

LIST OF FIGURES

LIST OF SYMBOLS AND ABBREVIATIONS

°	degree(s)
°C	degrees(s) celsius
Å	angstrom
α	alpha
β	beta
BF_4	tetrafluoroborate
Bu	butyl
CAAC	cyclic (alkyl)(amino) carbene
$CDCl_3$	chloroform-*d*
CH_2Cl_2	dichloromethane
d	doublet
γ	gamma
δ	delta, chemical shift
Et	ethyl
g	gram(s)

ICy	1,3-bis(cyclohexyl) imidazol-2-ylidene
IMes	1,3-bis(2,4,6-trimethylphenyl)imidazol-2-ylidene
IPr	1,3-bis(2,6-isopropyl-phenyl)imidazol-2-ylidene
I^{t}Bu	1,3-(di-*tert*-butyl)imidazol-2-ylidene
K	kelvin
L	ligand
MALDI	Matrix Assisted Laser Desorption/Ionization
M	metal
Me	methyl
MHz	megahertz
mmol	millimole(s)
mm	millimeter
μ	mu
NHC	N-heterocyclic carbene
NMR	nuclear magnetic resonance
$OSiMe_3$	silanolate
O^{t}Bu	tert-butoxide

OTf	trifluoromethanesulfonate or triflate
OTs	*p*-toluenesulfonate or tosylate
Ph	phenyl
ppm	parts per million
s	singlet
SIPr	1,3-bis(2,6-diisopropylphenyl)imidazolin-2-ylidene
sept	septet
T	temperature
t	triplet
THF	tetrahydrofuran

LIST OF SCHEMES

SUMMARY

This thesis describes the synthesis and structures of gold(I) sulfide and hydrosulfide complexes, supported by N-heterocyclic carbene (NHC) ligands. The first half of this thesis describes the synthesis of trigold(I) sulfide cations $\{[(ICy)Au]_3(\mu_3\text{-}S)\}^+$ and $\{[(IMes)Au]_3(\mu_3\text{-}S)\}^+$. The solid state structures of both of these complexes exhibit a pyramidal shape with the gold(I) atoms bridged by the sulfide. $\{[(ICy)Au]_3(\mu_3\text{-}S)\}^+$ was a dimeric complex that has some gold-to-gold distances within the range of a aurophilic interaction. On the other hand, $\{[(IMes)Au]_3(\mu_3\text{-}S)\}^+$ was a monomeric complex that has long gold−gold distances out of the range of a aurophilic interaction.

The second half of this thesis describes the synthesis of the terminal hydrosulfide gold(I) complex and the hydrosulfide-bridged gold(I) complex with IPr as a supporting ligand. Following the same procedure for the synthesis of ICy and IMes supported trigold sulfide complexes yielded a terminal hydrosulfide gold(I) complex when using IPr as a supporting ligand. The hydrosulfide-bridged gold(I) complex was prepared by the reaction between the terminal hydrosulfide gold(I) complex and $[LAu]^+$ cation.

CHAPTER 1. INTRODUCTION

1.1 Aurophilicity

Gold has several unique properties that influence the formation of coordination compouds. Most of the properties of gold compounds are rooted in their relativistic effects in the electron shells. When the net nuclear charge increases, the average velocity of the s electrons increases, which in turn increases mass of the atom. More importantly, the s orbital shrinks and shields the nuclear charge from the electrons in the d and f orbitals.[1] Electrons in the 6s orbital are more strongly bound to the nucleus while electrons in the 5d orbital are less strongly bound due to this relativistic contraction. This causes the 6s orbital size and energy to decrease while 5d orbital size and energy increase, which in turn strengthens gold-to-ligand bonding.[2-3] Due to the relativistic contractions, the diameter of gold(I) was found to be smaller than that of silver(I)[4] and gold−gold distances are often shorter than two van der Waals radii of a gold atom.[5] These gold-to-gold intra- and intermolecular d^{10} closed-shell interactions for gold(I), termed aurophilic interactions, can aggregate gold(I) compounds into polynuclear compounds.[6]

The aurophilic interaction or aurophilicity, first coined Schmidbaur,[7] is characterized by a gold−gold distance ranging from 2.7Å to 3.3Å. This gold−gold interaction has an enthalpy comparable to that of a hydrogen bond.[6, 8] Various reviews on aurophilicity show an expanding interest in the topic over the years[6-9] with applications in catalysis[10] and luminescent compounds.[11-13]

1.2 Isolobal Analogy of Gold (I) and H^+

The isolobal analogy, developed independently by Hoffmann[14] and Fukui,[15] relates molecular fragments when the shape, energy, and occupancy of the frontier orbitals are similar. The gold(I) cation and the proton have been considered isolobal based on the similarities between the Au 6s orbital and H 1s orbital. Small gold cluster ions such as Au_2^+ and Au_3^+ have been detected by mass spectrometry;[16-17] however, gold(I) complexes usually need a supporting ligand for stability. Therefore for $[LAu]^+$, the σ-symmetric hybrid orbitals, sp_z and sd_z^2, are considered as the bonding orbitals.

The isolobal concept was first applied to gold chemistry by Stone[18] and Mingos.[19] The analogy between gold(I) to H^+ and R^+ (carbocations) has led to main group, metalloid, and transition metal aurated compounds being studied.[20]

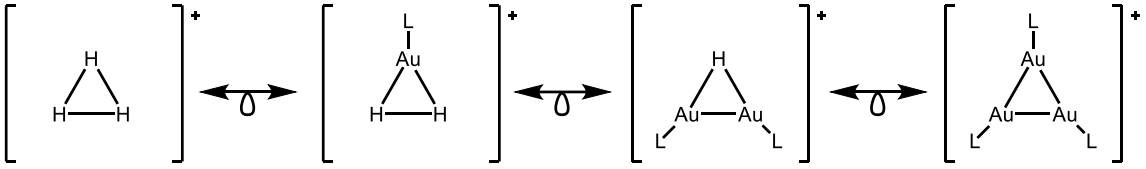

Figure 1.1. Isolobal analogy of H_3^+ to $(LAu)_3^+$.

Schmidbaur reviewed the isolobality topic on organogold complexes in 2012 and noted that the trinuclear cation $[(LAu)_3]^+$ (Figure 1.1) as well as the gold analogues of $[H_2I]^+$ and $[H_2F]^+$ had yet to be observed.[20] Within a couple of years, such complexes were synthesized using N-heterocyclic carbenes (NHCs) as ligands. Analogues of $[H_2F]^+$ were synthesized with gold, silver, and copper using 1,3-bis(2,6-diisopropylphenyl)imidazolin-2-ylidene (SIPr).[21] $[(LAu)_3]^+$ was successfully synthesized using IPr as a ligand. Its reaction with I_2 affords both LAuI and $[(LAu)_2I]^+$.[22]

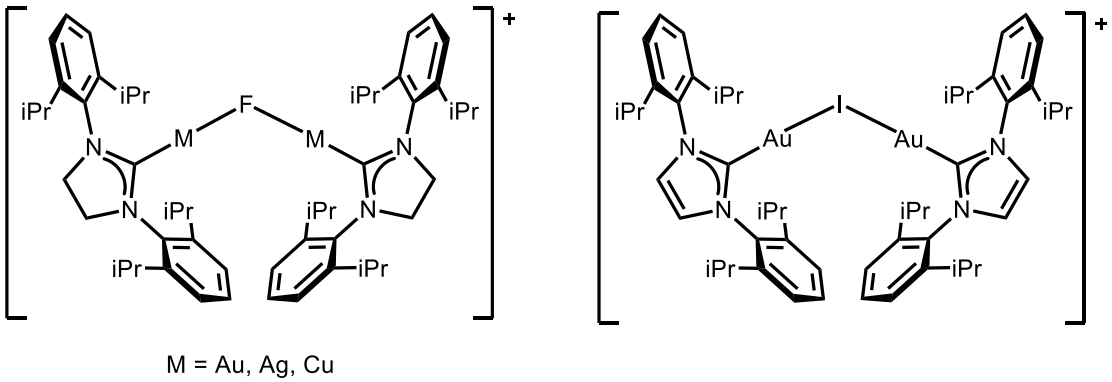

Figure 1.2. Fluoro-bridged coinage metal complexes with SIPr and iodo-bridged gold(I) complex with IPr.

Other coinage metal complexes based on the isolobal analogy of H_2 to MH and H_3^+ to $[M_2H]^+$ such as a terminal gold(I) hydride, and hydride-bridged dinuclear cations of gold(I),[23] silver(I),[24] and copper(I)[25] have been synthesized using NHCs as supporting ligands. These complexes show that NHCs as a stabilizing ligand are important for the stability of the compounds to form the central triangular core structure.

1.3 Gold Oxo Complexes

One of the early examples of a polynuclear gold complex was a trigold μ_3-oxo salt bearing triphenylphosphine as a ligand, $[(LAu)(\mu_3\text{-}O)]^+$, by Nesmayanov.[26] The synthetic route to this complex was later extended to a series of complexes by Sharp and co-workers using phosphine, phosphinite, and phosphite ligands.[27] The reaction of a (phosphine)gold(I) chloride or its analogues with silver(I) oxide gave rise to a stable pyramidal cation with three gold atoms clustering around an oxygen atom. The tendency of (phosphine)gold(I) cations to form polynuclear clusters is attributed to inter- and intramolecular aurophilic interactions. Depending on the phosphine ligands, the structure of the gold oxo complex differs. Less sterically hindered phosphine ligands such as

triphenylphosphine and methyldiphenylphosphine form a dimeric tris[(phosphine)gold(I)] oxo complex, whereas more sterically hindered phosphine ligands, such as tri(*o*-tolyl)phosphine, form monomers.[27] A hyper-aurated tetragold oxo dication has also been isolated by the addition of (tri(o-tolyl)phosphine)gold(I) tetrafluoroborate to tris[(tri(o-tolyl)phosphine)gold(I)] oxo tetrafluoroborate.[28]

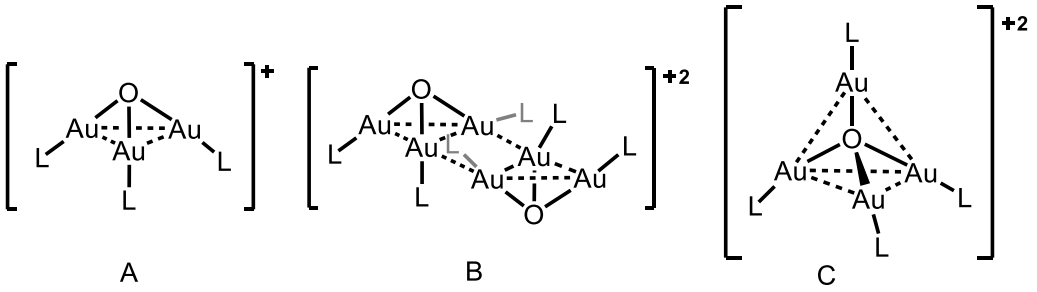

Figure 1.3. Structures of the oxogold species: monomer (A) and dimer (B); tetragold oxo dication (C).

The trigold oxo complexes exhibit interesting reactivity. The oxygen atom can be replaced with other chalcogenides[29-31] or with an amine.[32-33] This complex can also be reduced using carbon monoxide gas to form mixed-valent gold(I/0) clusters including, $[(LAu)_4]^{2+}$, $[(LAu)_6]^{2+}$, and $[L_6Au_8]^{2+}$.[34-35] This method became of interest to synthesize a smaller gold complex $[(LAu)_3]^+$ using NHCs as ligands instead of phosphines. Sadighi and co-workers used IPr (IPr = 1,3-bis(2,6-isopropyl-phenyl)imidazol-2-ylidene) as a ligand, but were unable to form the trigold oxo complex. However, they were able to synthesize the trigold monocation using a different route. A reaction of silanolate-bridged digold cation, $[(LAu)_2(\mu\text{-}OSiMe_3)]^+$, with $(LAu)OSiMe_3$ in CO_2 gas formed a μ_3-carbonate complex, which underwent reduction by CO gas. Another $[(LAu)_3]^+$ complex using cyclic (alkyl)(amino) carbene (CAAC) ligands was synthesized by the reduction of the

corresponding trigold oxo cation with CO gas.[36] In unpublished work, a sterically smaller NHC, I^{t}Bu (I^{t}Bu = 1,3-(di-*tert*-butyl)imidazol-2-ylidene) was found to support a trigold oxo complex, which underwent reduction to a trigold monocation; however, crystal formation had been unsuccessful, and a small amount of homoleptic byproduct $[L_2Au]^+$ could not be removed. Differences in steric hindrance between IPr and I^{t}Bu were thought to be the reason for the formation of the trigold oxo complex of the latter. Slightly sterically larger NHCs such as ICy and IMes were instead targeted for use; however, the use of these ligands did not enable the formation of the trigold oxo complex. Instead, the homoleptic complex, $[L_2Au]^+$, was formed following established procedures. To better incorporate larger NHC ligands, the chalcogen center was switched from oxygen to sulfur.

Compared to gold-oxygen bonds, bond distance between gold and sulfur are longer and expected to better incorporate larger NHCs. Sulfide donors are also a softer base compared to oxygen donors according to hard and soft acids and bases theory (HSAB)[37] and would be a better match to a gold(I) soft acid. This should mitigate the formation of the homoleptic complex and enable the formation of a trigold(I) sulfide complex. This route using trigold(I) sulfide complexes were explored as possible synthons for previously inaccessible trigold monocations.

1.4 References

1. Bartlett, N., *Gold Bull.* **1998,** *31*, 22-25.
2. Gorin, D. J.; Toste, F. D., *Nature* **2007,** *446*, 395-403.
3. Pyykkö, P., *Chem. Soc. Rev.* **2008,** *37*, 1967-1997.
4. Bayler, A.; Schier, A.; Bowmaker, G. A.; Schmidbaur, H., *J. Am. Chem. Soc.* **1996,** *118*, 7006-7007.

5. Rahm, M.; Hoffmann, R.; Ashcroft, N. W., *Chem. Eur. J.* **2016,** *22*, 14625-14632.

6. Schmidbaur, H., *Gold Bull.* **2000,** *33*, 3-10.

7. Schmidbaur, H., *Gold Bull.* **1990,** *23*, 11-21.

8. Schmidbaur, H.; Schier, A., *Chem. Soc. Rev.* **2008,** *37*, 1931-1951.

9. Schmidbaur, H.; Schier, A., *Chem. Soc. Rev.* **2012,** *41*, 370-412.

10. Weber, D.; Gagné, M. R., *Top. Curr. Chem.* **2015,** *357*, 167-211.

11. Fernandez, E. J.; Laguna, A.; Lopez-de-Luzuriaga, J. M., *Dalton Trans.* **2007**, 1969-1981.

12. McDougald, R. N., Jr.; Chilukuri, B.; Jia, H.; Perez, M. R.; Rabaa, H.; Wang, X.; Nesterov, V. N.; Cundari, T. R.; Gnade, B. E.; Omary, M. A., *Inorg. Chem.* **2014,** *53*, 7485-7499.

13. Melgarejo, D. Y.; Chiarella, G. M.; Fackler, J. P., Jr., *Inorg. Chem.* **2016,** *55*, 11883-11889.

14. Hoffmann, R., *Angew. Chem. Int. Ed.* **1982,** *21*, 711-724.

15. Fukui, K., *Science* **1982,** *218*, 747-754.

16. Moini, M.; Eyler, J. R., *Chem. Phys. Lett.* **1987,** *137*, 311-314.

17. Moini, M.; Eyler, J. R., *J. Chem. Phys.* **1988,** *88*, 5512-5515.

18. Stone, F. G. A., *Angew. Chem. Int. Ed.* **1984,** *23*, 89-99.

19. Mingos, D. M. P., *J. Chem. Soc., Dalton Trans.* **1976**, 1163-1169.

20. Raubenheimer, H. G.; Schmidbaur, H., *Organometallics* **2012,** *31*, 2507-2522.

21. Wyss, C. M.; Tate, B. K.; Bacsa, J.; Wieliczko, M.; Sadighi, J. P., *Polyhedron* **2014,** *84*, 87-95.

22. Robilotto, T. J.; Bacsa, J.; Gray, T. G.; Sadighi, J. P., *Angew. Chem. Int. Ed.* **2012,** *51*, 12077-12080.

23. Tsui, E. Y.; Muller, P.; Sadighi, J. P., *Angew. Chem. Int. Ed.* **2008,** *47*, 8937-8940.

24. Tate, B. K.; Wyss, C. M.; Bacsa, J.; Kluge, K.; Gelbaum, L.; Sadighi, J. P., *Chem. Sci.* **2013,** *4*, 3068-3074.

25. Wyss, C. M.; Tate, B. K.; Bacsa, J.; Gray, T. G.; Sadighi, J. P., *Angew. Chem. Int. Ed.* **2013,** *52*, 12920-12923.

26. Nesmeyanov, A. N.; Perevalova, E. G.; Struchkov, Y. T.; Antipin, M. Y.; Grandberg, K. I.; Dyadhenko, V. P., *J. Organomet. Chem.* **1980,** *201*, 343-349.

27. Yang, Y.; Ramamoorthy, V.; Sharp, P. R., *Inorg. Chem.* **1993,** *32*, 1946-1950.

28. Schmidbaur, H.; Hofreiter, S.; Paul, M., *Nature* **1995,** *377*, 503-504.

29. Angermaier, K.; Schmidbaur, H., *Chem. Ber.* **1994,** *127*, 2387-2391.

30. Crespo, O.; Gimeno, M. C.; Laguna, A.; Larraz, C.; Villacampa, M. D., *Chem. Eur. J.* **2007,** *13*, 235-246.

31. Angermaier, K.; Schmidbaur, H., *Z. Naturforsch. B* **1996,** *51*, 879-882.

32. Lange, P.; Beruda, H.; Hiller, W.; Schmidbaur, H., *Z. Naturforsch. B* **1994,** *49b*, 781-787.

33. Sharp, P. R.; Yi, Y.; Wu, Z.; Ramamoorthy, V., Gold Oxo, Imido, and Hydrazido complexes and Gold Clusters. In *The chemistry of the copper and zinc triads*, Welch, A. J.; Chapman, S. K., Eds. Cambridge : Royal Society of Chemistry: Cambridge, 1993; pp 198-201.

34. Ramamoorthy, V.; Wu, Z.; Yi, Y.; Sharp, P. R., *J. Am. Chem. Soc.* **1992,** *114*, 1526-1527.

35. Yang, Y.; Sharp, P. R., *J. Am. Chem. Soc.* **1994,** *116*, 6983-6984.

36. Jin, L.; Weinberger, D. S.; Melaimi, M.; Moore, C. E.; Rheingold, A. L.; Bertrand, G., *Angew. Chem. Int. Ed.* **2014,** *53*, 9059-9063.

37. Pearson, R. G., *J. Am. Chem. Soc.* **1963,** *85*, 3533-3539.

CHAPTER 2. SYNTHESIS OF N-HETEROCYCLIC CARBENE TRIGOLD SULFIDE COMPLEXES

2.1 Background

Sulfide- and other chalcogenide-centered gold clusters bearing various phosphorous based ligands have been previously synthesized and studied.[1] Among the earliest examples of a (phosphine)gold(I) sulfide complex were the trigold(I) μ_3-sulfide cation and the neutral di(phosphine)gold(I) μ_2-sulfide reported in 1966 by Kowala and Swan.[2] It was not until much later when (phosphine)gold sulfide complexes were explored further, and synthetic procedures were established. Schmidbaur and co-workers synthesized the trigold sulfide cation from $[(R_3PAu)_3(\mu_3\text{-}O)]^+$ or $[(R_3P)Au]BF_4$ by addition of $S(SiMe_3)_2$.[3] Another synthetic pathway involved a bridged-phosphanyl ligand, 1,3,5-tris[(diphenylphosphanyl)methyl]trimethyl benzene, supported gold(I) chloride complex reaction with sodium sulfide (Figure 2.1 A).[4]

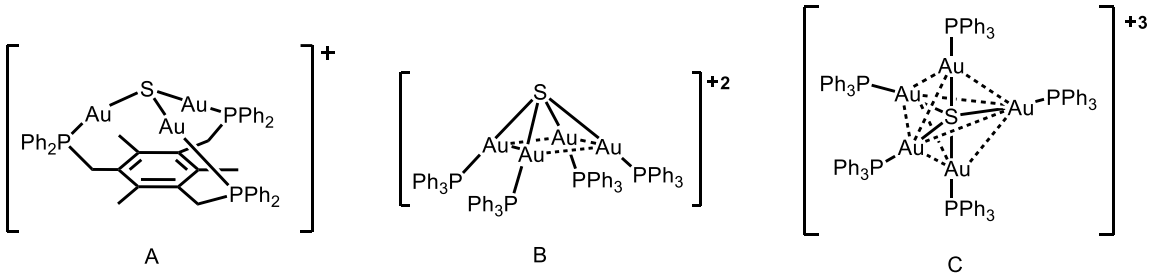

Figure 2.1. Structures of 1,3,5-tris[(diphenylphosphanyl)methyl]trimethylbenzene supported trigold(I) sulfide (A), tetrakis[(triphenylphosphine)gold(I)] sufide (B), pentakis[(triphenylphosphine)gold(I)] sufide (C).

Sulfide-centered gold clusters have been studied with various phosphorous containing ligands by the Gimeno group.[5-9] Synthesis of a larger polyaurated species was possible by the stoichiometric addition of (phosphine)gold(I) cation to a di(phosphine)gold(I) sulfide. The di(phosphine)gold(I) sulfide was synthesized by reaction of two equivalents of (phosphine)gold(I) chloride with lithium sulfide using phosphine ligands such as triphenylphosphine[5] and 1,1'-bis(diphenylphosphino)ferrocene (dppf).[7] Triphenylphosphine was found to support clusters ranging from dinuclear to hexanuclear (Figure 2.1 B,C). Other phosphine ligands could be incorporated into a gold sulfide cluster, such as tris(*m*-tolyl)phosphine, and tri(*p*-tolyl)phosphine, by stoichiometric addition of (phosphine)gold(I) triflate to the di(phosphine)gold(I) sulfide complex to form polyaurated sulfide clusters.[6]

Compared to (phosphine)gold complexes, there are relatively few examples of (NHC)-supported gold sulfide complexes. Sadighi and co-workers synthesized a benzenethiolate-bridged digold(I) cation and terminal gold(I) benzenethiolate from the addition of excess benzenethiol to $[(IPr)Au]_3OTf$.[10] An unusual octanuclear NHC coinage metal cluster $[(IPr)Au]_4(\mu_3\text{-}E)_4M_4$ (M=Au or Ag) with luminescent properties was synthesized using (NHC)-gold(I) trimethylsilylchalcogenolates (E = S, Se, Te) as a starting material.[11] A tricopper(I) sulfide complex, $\{[(IPr)Cu]_3(\mu_3\text{-}S)\}BF_4$, was synthesized by the addition of two $(IPr)Cu^+$ synthons to $(IPr)CuSSiMe_3$.[12] A bridging trimethylsilyl thiolato complex was first formed by a reaction between $(IPr)CuSSiMe_3$ and $[(IPr)Cu(NCMe)]BF_4$, then (IPr)CuF was added to form the tricopper(I) sulfide complex.

This chapter describes the synthesis of the trinuclear gold(I) sulfide complexes $\{[(ICy)Au]_3(\mu_3\text{-}S)\}X$ [ICy = 1,3-bis(cyclohexyl) imidazol-2-ylidene; X^- = Cl^-, BF_4^-, or

OTs^- (tosylate, 4-$CH_3C_6H_4SO_3^-$)] and {[(IMes)Au]$_3$(μ_3-S)}BF_4. [IMes = 1,3-bis(2,4,6-trimethylphenyl)imidazol-2-ylidene] under ambient conditions using a similar procedure.[4] Structural data show the cations adopting a trigonal pyramidal shape. The Au−Au distances differ with each NHC ligand. These complexes were shown to be air and moisture stable.

2.2 Results and Discussion

2.2.1 Synthesis and Structural Characterization of {[(ICy)Au]$_3$(μ_3-S)}X and {[(IMes)Au]$_3$(μ_3-S)}BF_4 Salts

The trigold μ_3-sulfide cations were obtained as their chloride salts by mixing (ICy)gold(I) chloride or (IMes)gold(I) chloride with excess technical grade sodium sulfide nonahydrate in 200 proof ethanol (Scheme 2.1). Anion exchange was achieved by stirring in a biphasic mixture of dichloromethane and distilled water with either sodium tetrafluoroborate ($NaBF_4$) or sodium *p*-toluenesulfonate (NaOTs).

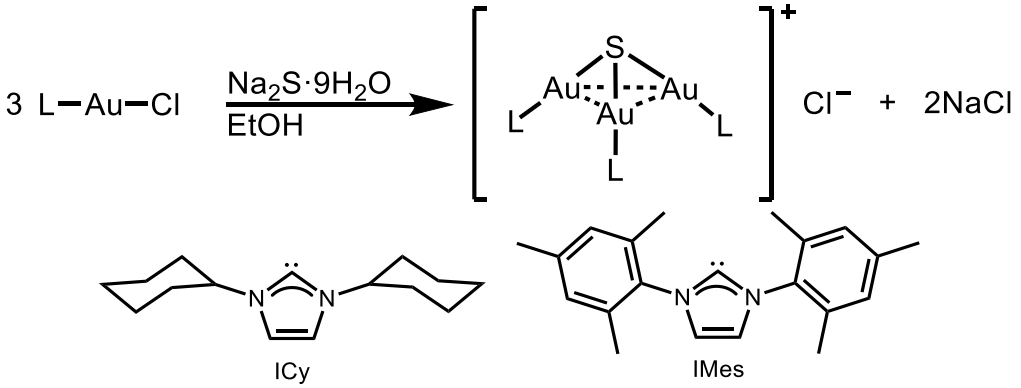

Scheme 2.1. Synthesis of NHC trigold sulfide. L = ICy or IMes.

The ^{1}H NMR spectra of {[(ICy)Au]$_3$(μ_3-S)}Cl and {[(ICy)Au]$_3$(μ_3-S)}BF_4 show a single set of ICy resonances, however, this observation does not indicate the nuclearity of the compound. Therefore, a counteranion with ^{1}H NMR signals was used for anion exchange.

The ^{1}H NMR spectrum of {[(ICy)Au]$_3$(μ_3-S)}OTs shows a set of ICy resonances and tosylate resonances corresponding to a 3:1 ratio. Mass spectrometry with MALDI shows *m/z* = 1319.35, matching with the {[(ICy)Au]$_3$(μ_3-S)}$^+$ ion. The ^{1}H NMR spectrum of {[(IMes)Au]$_3$(μ_3-S)}BF_4 shows a single set of IMes resonances. Analysis of the {[(IMes)Au]$_3$(μ_3-S)}$^+$ cation by MALDI-MS was in agreement with the expected formula with *m/z* = 1535.38. {[(IMes)Au]$_3$(μ_3-S)}Cl could not be isolated pure as there was some (IMes)AuCl detected by ^{1}H NMR spectroscopy. A tetrafluoroborate salt of {[(IMes)Au]$_3$(μ_3-S)}$^+$ was obtained by pure ion exchange followed by recrystallization.

2.2.2 X-ray Crystal Structure of {[(ICy)Au]$_3$(μ_3-S)}OTs

Vapor diffusion of hexanes into a dichloromethane solution of {[(ICy)Au]$_3$(μ_3-S)}OTs afforded clear colorless crystals suitable for single crystal X-ray diffraction. {[(ICy)Au])$_3$(μ_3-S)}OTs formed a dimeric structure similar to that observed for certain tris[(phosphine)gold] oxo[13] and sulfide salts.[3, 6] However, unlike the phosphine analogues, each monomer of {[(ICy)Au]$_3$(μ_3-S)}$^+$ was not perfectly C_{3v} symmetric and the dimer itself was not symmetric (Figure 2.2). The Au–Au distances within the monomer range from 3.0778(12) Å to 3.400(1) Å. The Au(1)–Au(3) and Au(3)–Au(2) bonds lengths are within the distance generally accepted for an aurophilic interaction,[14] however, the Au(1)–Au(2) distance is not. Due to the different Au–Au distances, Au–S–Au bond angles range from 83.9(2)° to 95.1(2)°. The closest Au–Au distances between each monomer, Au(1)-Au(1) and Au(2)-Au(2), are inequivalent at 2.9580(18) and 3.523(2) Å.

The Au–S distances are all close to 2.30 Å, slightly shorter than those in (phosphine)gold sulfide clusters. The Au−C_{NHC} bond lengths are in agreement with those

in other gold carbene complexes[15] and theoretically calculated values for various other NHC gold complexes.[16]

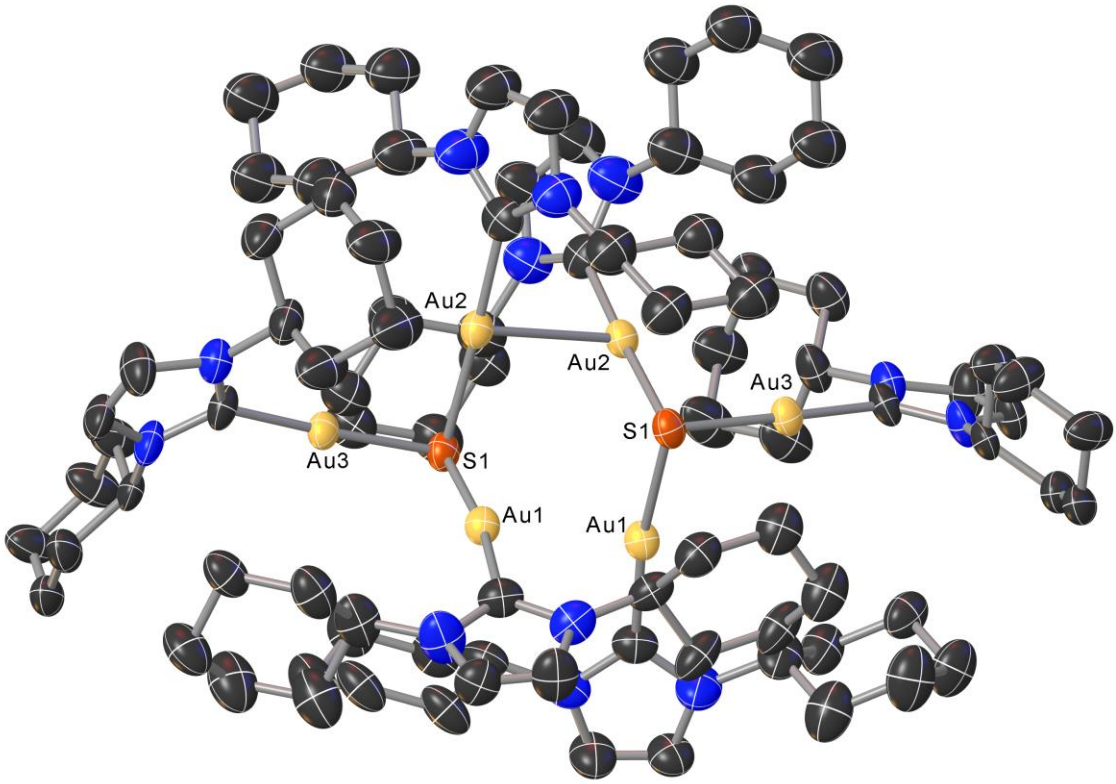

Figure 2.2. Solid state structure of {[(ICy)Au]$_3$(μ$_3$-S)}OTs. Anion and hydrogens omitted for clarity. Selected interatomic distances (Å) and angles (°): Au(1)−S(1), 2.298(6); Au(2)−S(1), 2.309(6); Au(3)−S(1), 2.294(6); Au(1)−Au(2), 3.400(1); Au(2)−Au(3), 3.0778(12); Au(1)−Au(3), 3.1922(12); Au(1)−Au(1), 3.523(2); Au(2)−Au(2), 2.9580(18); Au(1)−S(1)−Au(2), 95.1(2); Au(2)−S(1)−Au(3), 83.9(2); Au(1)−S(1)−Au(3), 88.1(2).

2.2.3 X-ray Crystal Structure of {[(IMes)Au]$_3$(μ$_3$-S)}Cl

Using procedures similar to those for {[(ICy)Au]$_3$(μ$_3$-S)}OTs, vapor diffusion of hexane into a dichloromethane solution of {[(IMes)Au]$_3$(μ$_3$-S)}Cl afforded clear colorless crystals suitable for single crystal X-ray diffraction. In contrast to {[(ICy)Au]$_3$(μ$_3$-S)}OTs, {[(IMes)Au]$_3$(μ$_3$-S)}Cl was a monomer with approximate C_{3v} symmetry, but with longer Au–Au distances of 3.5208(4) Å to 3.5226(4) Å. These distances are longer than those

normally considered to involve aurophilic interactions (Figure 2.3). The Au–S and Au–C_{NHC} distances are similar to those in {[(ICy)Au]$_3$(μ_3-S)}OTs. The trigonal pyramidal shape of the molecule was flatter, and the Au–S–Au bond angles are almost uniform ranging from 99.73(4)° and 99.77(4)°.

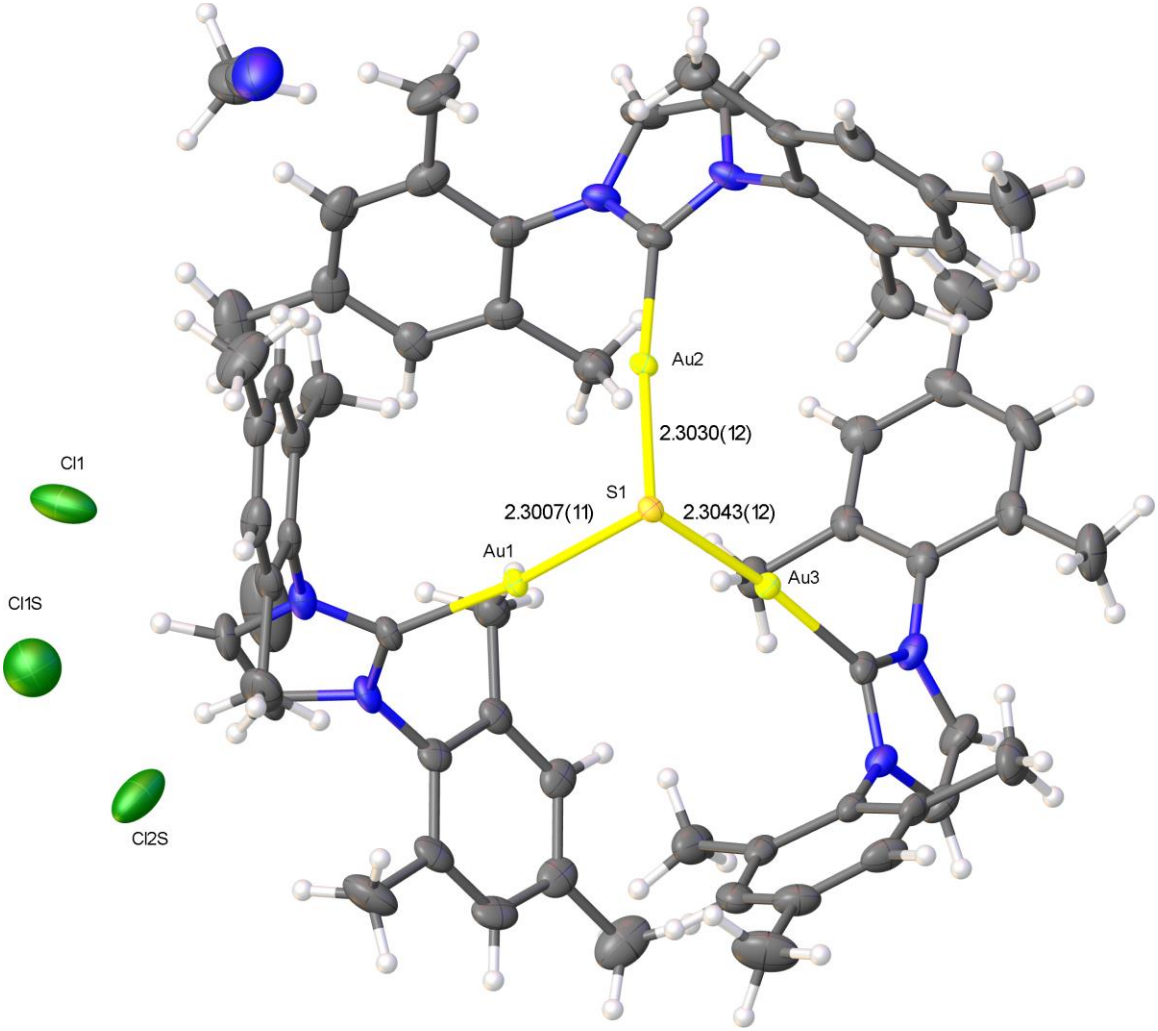

Figure 2.3. Solid state structure of {[(IMes)Au]$_3$(μ_3-S)}Cl. Selected interatomic distances (Å) and angles (°): Au(1)−S(1), 2.3007(14); Au(2)−S(1), 2.3032(12); Au(3)−S(1), 2.3043(12); Au(1)−Au(2), 3.5208(4); Au(2)−Au(3), 3.5226(4); Au(1)−Au(3), 3.5216(3); Au(1)−S(1)−Au(2), 99.7(4); Au(2)−S(1)−Au(3), 99.73(4); Au(1)−S(1)−Au(3), 99.7(4).

2.3 Conclusion

The sulfide-centered trigold cation was synthesized using the NHCs IMes and ICy as supporting ligands. Both complexes have a pyramidal core. {[(ICy)Au]$_3$(μ_3-S)}OTs was dimeric while the {[(IMes)Au]$_3$(μ_3-S)}Cl was monomeric in the solid state. The Au−Au distances were not uniform for {[(ICy)Au]$_3$(μ_3-S)}OTs in the solid state, causing the pyramidal shape to be distorted. The solid state structure of {[(IMes)Au]$_3$(μ_3-S)}Cl shows a symmetric complex; however, there were no indication of aurophilic interactions between the gold atoms. Both complexes were stable in air and moisture.

2.4 Experimental

2.4.1 General Considerations

Unless otherwise indicated, manipulations carried out in a fumehood under ambient conditions. Sodium sulfide hydrate, technical grade (Alfa Aesar), sodium tetrafluoroborate (Alfa Aesar), sodium *p*-toluenesulfonate (TCI), 1,3-dicyclohexylimidazolium chloride (Sigma-Aldrich) and Celite (EMD 545) were used as received. Dichloromethane (BDH), ethanol (200 proof, KOPTEC), and pentane (EMD) solvents were used as received. IMes•HCl,[17] (IMes)AuCl, and (ICy)AuCl[18] were synthesized according to literature preparations and characterized by ^{1}H NMR spectroscopy.

^{1}H NMR and ^{13}C NMR spectra were acquired on a Varian Vx 400 MHz spectrometer and a Bruker Avance IIIHD 700 MHz spectrometer. ^{1}H NMR and ^{13}C NMR chemical shifts were referenced with respect to solvent signals relative to tetramethylsilane.[19] Chloroform-*d* (Cambridge Isotope Laboratories) was dried over activated molecular sieves (Alfa Aesar, 4Å).

Mass spectrometric analyses were carried out by David Bostwick using a Bruker AutoFlex III.

Elemental analyses were performed by Atlantic Microlab, Inc. in Norcross, Georgia.

2.4.2 Synthetic Procedures

{[(ICy)Au]$_3$(μ$_3$-S)}Cl. (ICy)AuCl (0.1001 g, 0.2154 mmol) was stirred in ethanol (5 mL, 200 proof) to produce a white, cloudy reaction mixture. $Na_2S \cdot nH_2O$ flakes (0.0258 g, 0.107 mmol assuming n=9) were added and the mixture was sonicated to break up the flakes. The solution was stirred for 6 hours. Ethanol was removed *in vacuo* and the white/yellow solid was redissolved in CH_2Cl_2. The redissolved mixture was filtered through a plug of Celite, concentrated, and the product was precipitated with the addition of pentane. The white solid was filtered and vacuum-dried. The solid was recrystallized with CH_2Cl_2 layered with pentane to afford the title complex as white crystals (0.0940 g, 95% yield). ^{1}H NMR (400 MHz, $CDCl_3$): δ (ppm) 7.11 (s, 2H, NC*H*), 4.55 (tt, *J* = 12.0, 3.8 Hz, 2H, C*H*), 2.08-1.17 (m, 20H, CH_2). ^{13}C NMR (100 MHz, $CDCl_3$): δ (ppm) 177.1 (N*C*Au), 117.5 (N*C*H), 60.9 (*C*H), 34.2 (*C*H_2), 25.5 (*C*H_2), 25.1 (*C*H_2). Anal. calcd for $C_{45}H_{72}Au_3ClN_6S$: C, 39.87; H, 5.35; N, 6.20. Found C, 38.92; H, 5.38; N, 6.04. MALDI(+): 1319.41 [M^+]

Note: A satisfactory elemental analysis was not obtained for this compound; however, it was suitable for the preparation of {[(ICy)Au]$_3$(μ$_3$-S)}BF_4 and {[(ICy)Au]$_3$(μ$_3$-S)}OTs.

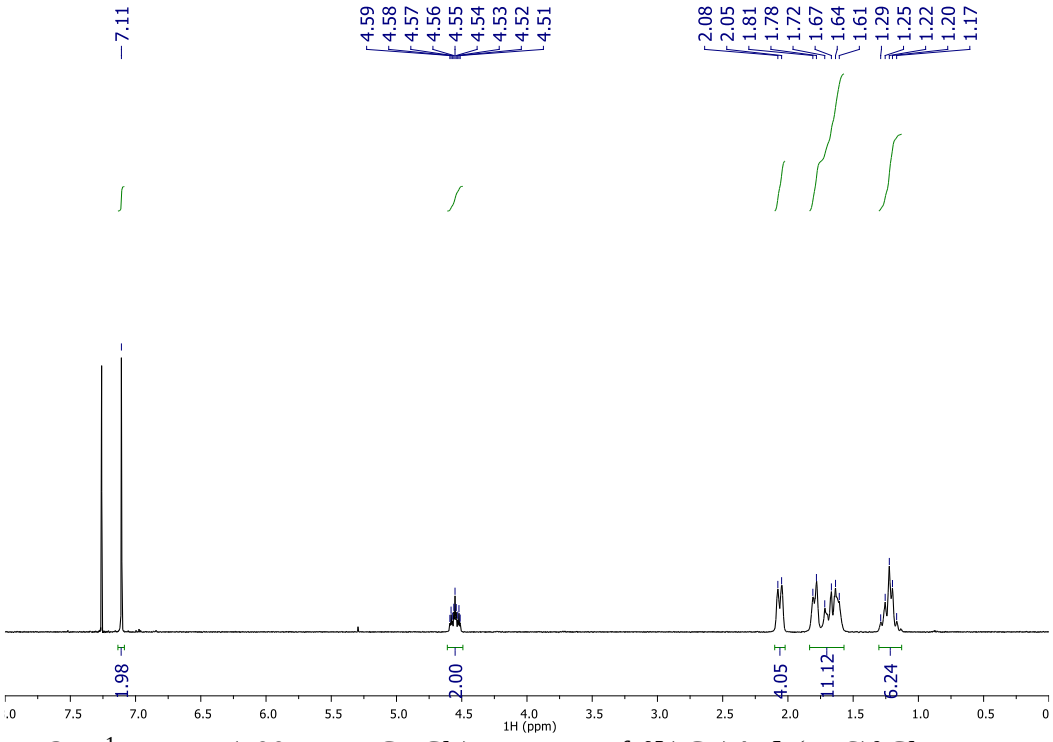

Figure 2.4. ^{1}H NMR (400 MHz, $CDCl_3$) spectrum of {[(ICy)Au]$_3$(μ_3-S)}Cl.

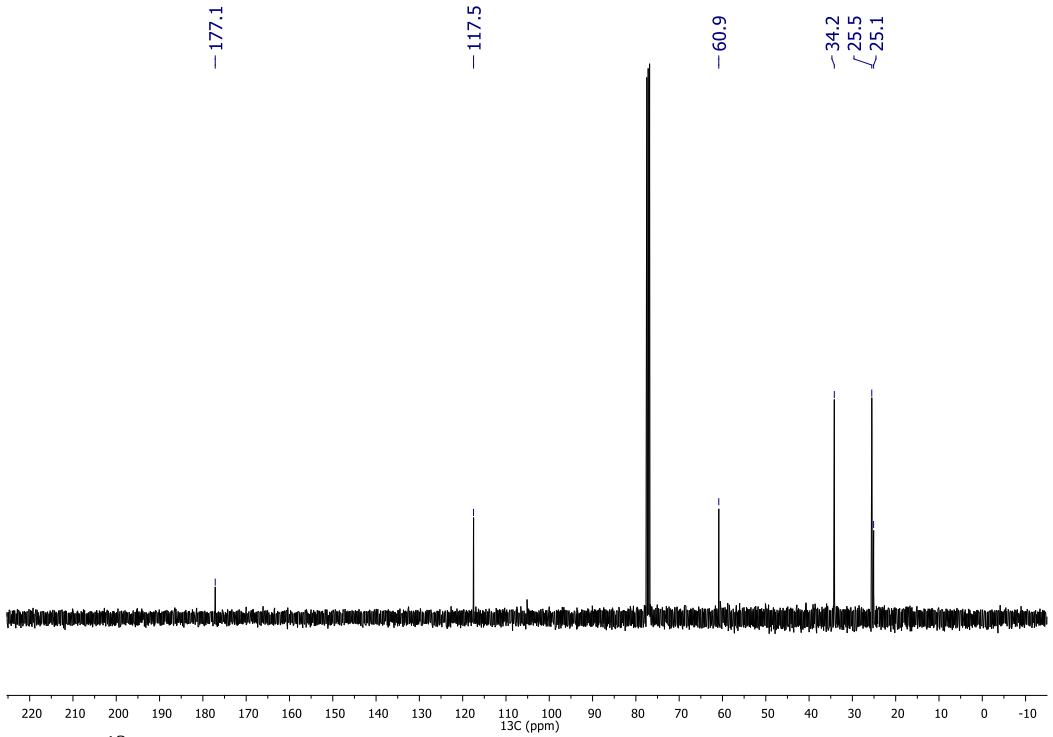

Figure 2.5. ^{13}C NMR (100 MHz, $CDCl_3$) spectrum of {[(ICy)Au]$_3$(μ_3-S)}Cl.

{[(ICy)Au]$_3$(μ$_3$-S)}BF$_4$. **{**[(ICy)Au]$_3$(μ$_3$-S)}Cl (0.0578 g, 0.0427 mmol) and excess NaBF$_4$ (0.0119 g, 0.3146 mmol) were mixed in a biphasic mixture of CH_2Cl_2 and distilled H_2O, and stirred for 1 hour. The CH_2Cl_2 layer was decanted and the solvent was removed in vacuo to yield a white solid. The solid was recrystallized with CH_2Cl_2 layered with pentane to yield white crystals (0.0551 g, 92%). ^{1}H NMR (400 MHz, $CDCl_3$): δ (ppm) 7.06 (s, 2H, NC*H*), 4.54 (tt, *J* = 12.0, 3.8 Hz, 2H, C*H*), 2.07-1.16 (m, 20H, CH_2). ^{13}C NMR (176 MHz, CDCl3): δ (ppm) 177.1 (N*C*Au), 117.4 (N*C*H), 60.9 (*C*H), 34.1 (*C*H$_2$), 25.5 (*C*H$_2$), 25.1 (*C*H$_2$). Anal. calcd for $C_{45}H_{72}Au_3BF_4N_6S$: C, 38.42; H, 5.16; N, 5.97. Found C, 38.45; H, 5.13; N, 5.98.

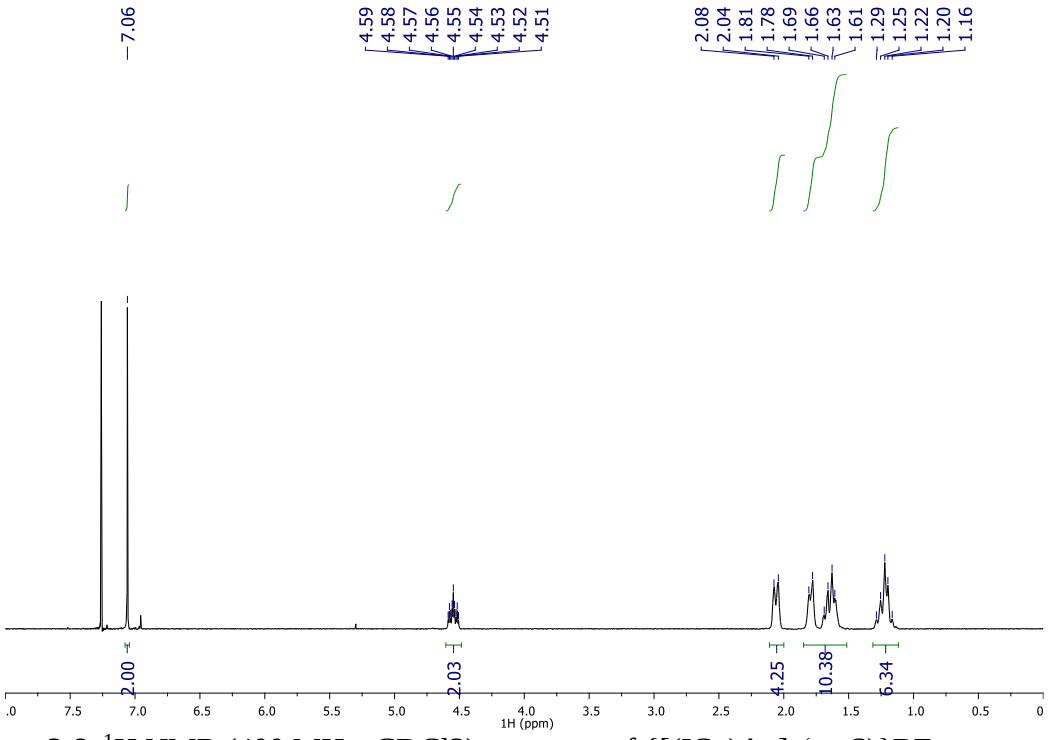

Figure 2.6. ^{1}H NMR (400 MHz, CDCl3) spectrum of {[(ICy)Au]$_3$(μ$_3$-S)}BF$_4$.

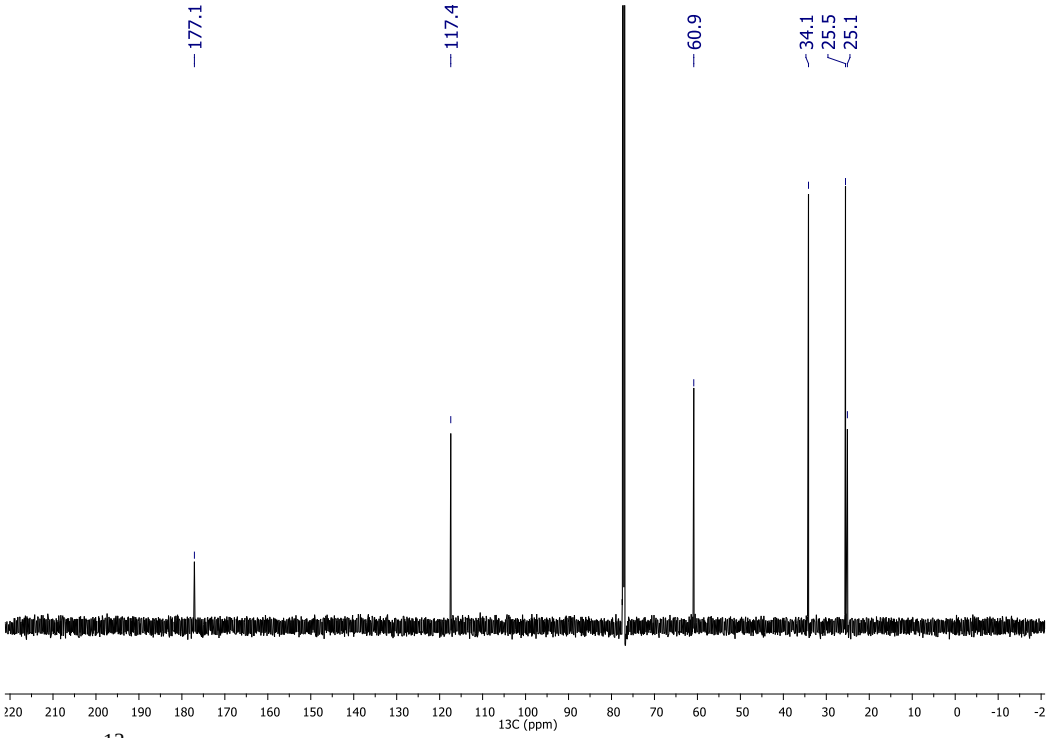

Figure 2.7. ^{13}C NMR (176 MHz, CDCl3) spectrum of {[(ICy)Au]$_3$(μ$_3$-S)}BF$_4$.

{[(ICy)Au])$_3$(μ$_3$-S)}OTs. {[(ICy)Au]$_3$(μ$_3$-S)}Cl (0.0504 g, 0.0372 mmol) and excess sodium tosylate (0.0154 g, 0.0793 mmol) were mixed in a biphasic mixture of CH_2Cl_2 and distilled H_2O for 1 hour. The CH_2Cl_2 layer was decanted and the solvent was removed *in vacuo* to yield a white solid. The solid was recrystallized with CH_2Cl_2 layered with pentane to yield white crystals (0.0515 g, 93%). Crystals suitable for X-ray diffraction were grown by slow diffusion of hexane into the complex dissolved in a solution of CH_2Cl_2. ^{1}H NMR (400 MHz, $CDCl_3$): δ (ppm) 7.89 (d, J = 8.2 Hz, 2H, C*H*$_{Ar}$), 7.09 (s, 6H, NC*H*), 7.08 (d, 2H, C*H*$_{Ar}$), 4.53 (tt, J = 12.1, 3.9 Hz, 6H, C*H*), 2.29 (s, 3H, C*H*$_3$), 2.13 – 1.09 (m, 60H, C*H*$_2$). ^{13}C NMR (176 MHz, CDCl3) δ 177.0 (N*C*Au), 145.1 (*C*$_{Ar}$), 138.1 (*C*$_{Ar}$), 128.3 (*C*$_{Ar}$), 126.6 (*C*$_{Ar}$), 117.6 (N*C*H), 60.8 (*C*H), 34.2 (*C*H$_2$), 25.5 (*C*H$_2$), 25.1 (*C*H$_2$), 21.4 (*C*H$_3$). Anal. calcd for $C_{52}H_{79}Au_3N_6O_3S_2$: C, 41.88; H, 5.34; N, 5,64. Found C, 42.04; H, 5.49; N, 5.61.

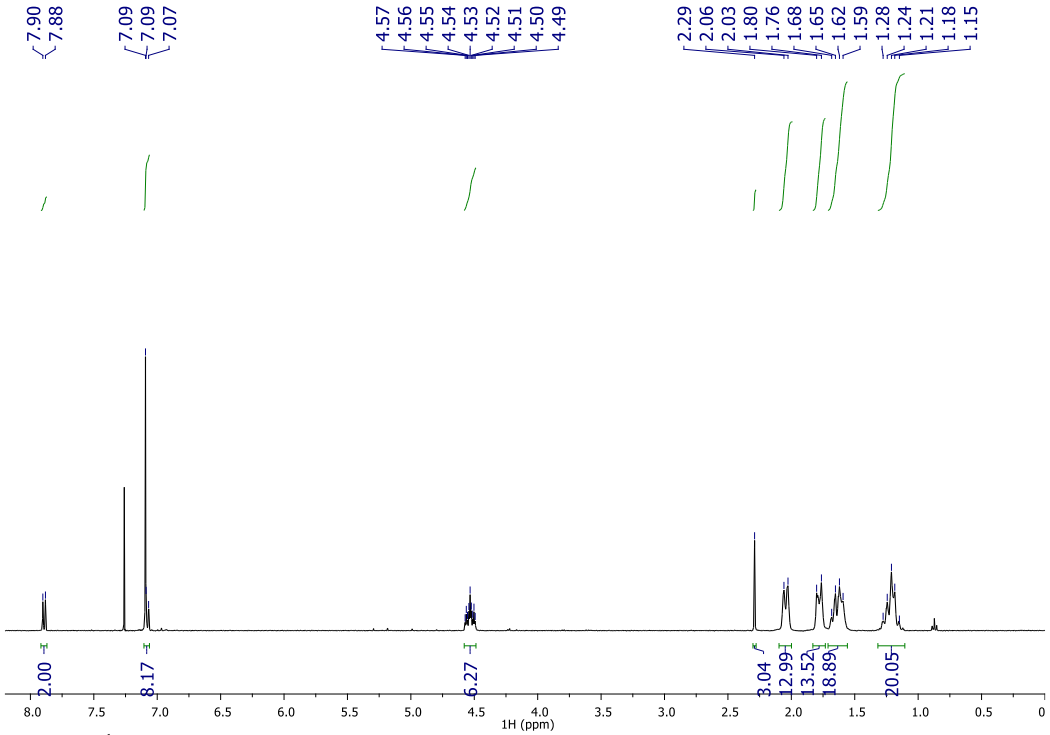

Figure 2.8. ^{1}H NMR of (400 MHz, $CDCl_3$) spectrum of {[(ICy)Au]$_3$(μ_3-S)}OTs. Trace of pentane at δ 0.87 ppm.

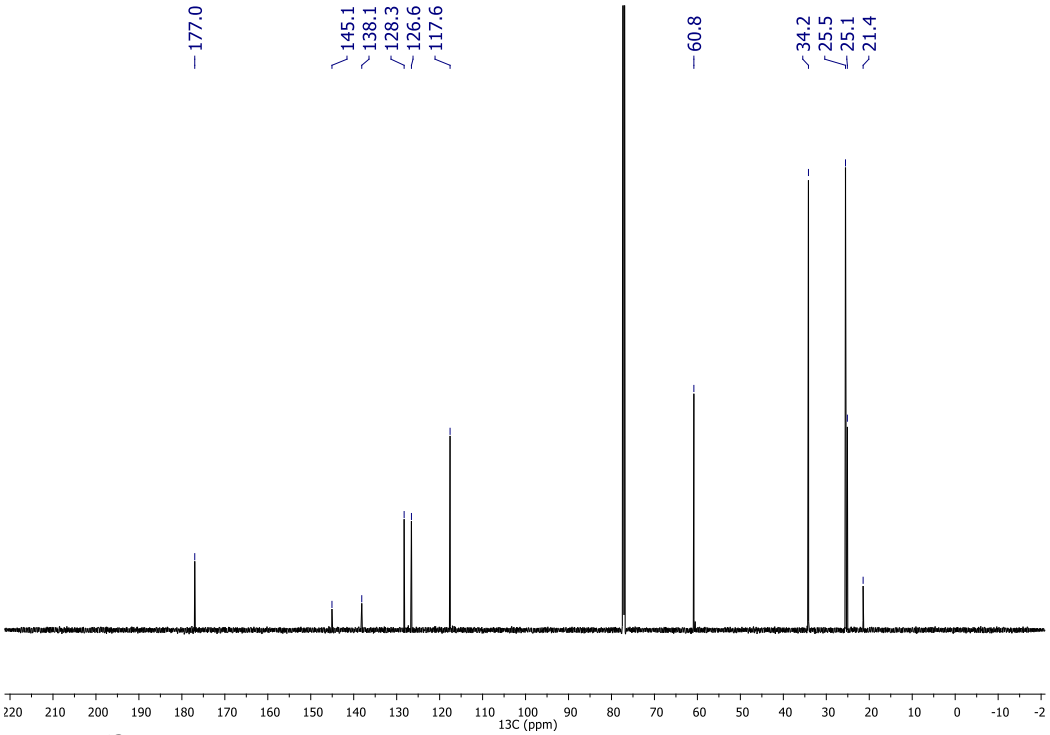

Figure 2.9. ^{13}C NMR (176 MHz, $CDCl_3$) spectrum of {[(ICy)Au]$_3$(μ_3-S)}OTs.

{[(IMes)Au]$_3$(μ$_3$-S)}BF$_4$. (IMes)AuCl (0.0500 g, 0.0931 mmol) and an excess of $Na_2S \cdot nH_2O$ flakes (0.0303 g, 0.1262 mmol assuming n=9) were stirred in ethanol (5 mL, 200 proof). The solution was briefly sonicated to break apart Na_2S flakes. After 6 hours of stirring, the ethanol was removed *in vacuo* and the solid was dissolved in CH_2Cl_2 (~5 mL). The CH_2Cl_2 solution was filtered through a plug of Celite, which was then washed with additional CH_2Cl_2 (2 mL). $NaBF_4$ (8.2 mg, 0.0747 mmol) and distilled H_2O (2 mL) were added and the biphasic mixture was stirred for 1.5 hours. The CH_2Cl_2 layer was decanted and the solvent was removed *in vacuo* to yield a white solid. The solid was recrystallized with CH_2Cl_2 layered with pentane to yield white crystals (0.0437 g, 87%). ^{1}H NMR (400MHz, $CDCl_3$): δ (ppm) 7.02 (s, 2H, NC*H*) 6.88 (s, 4H, CH_{Ar}), 2.29 (s, 6H, CH_3), 1.93 (s, 12H, CH_3). ^{13}C NMR (176 MHz, $CDCl_3$): δ (ppm) 181.6 (N*C*Au), 139.2 (*C*$_{Ar}$), 134.9 (*C*$_{Ar}$), 134.6 (*C*$_{Ar}$), 129.4 (*C*$_{Ar}$), 122.6 (N*C*H), 21.3 (*C*H$_3$), 18.0 (*C*H$_3$). Anal. calcd for $C_{63}H_{72}Au_3BF_4N_6S$: C, 46.62; H, 4.47; N, 5.18. Found C, 46.46; H, 4.56; N, 5.19.

Note: ^{13}C NMR assignment of the imidazolylidene backbone carbons are tentative.

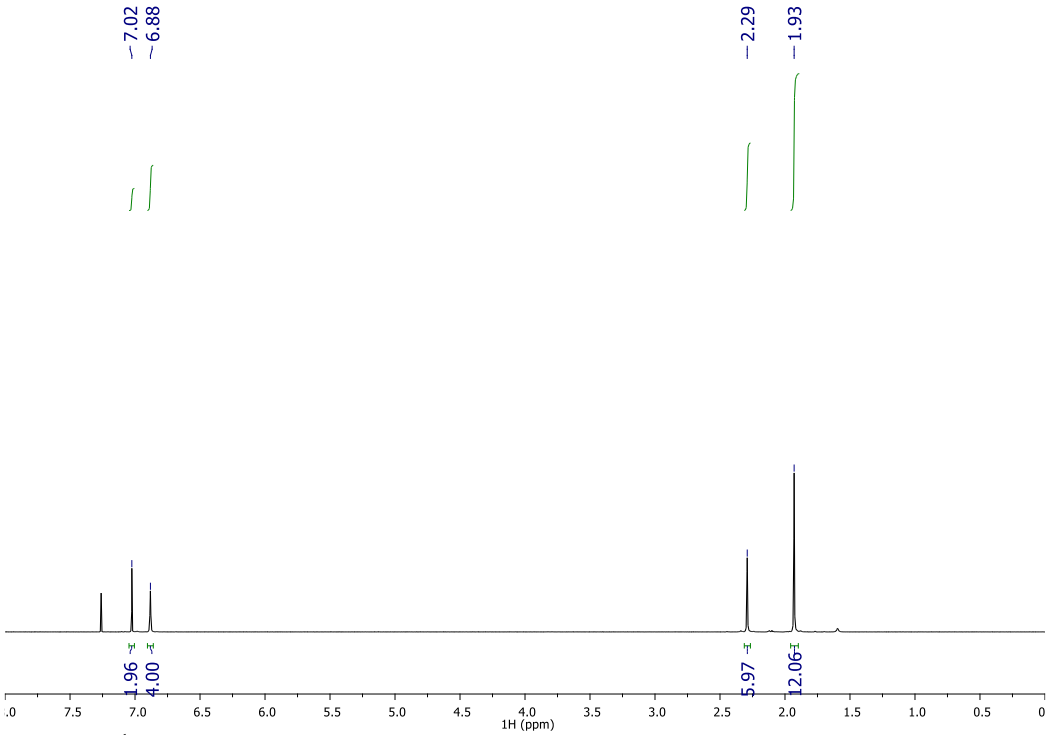

Figure 2.10. ^{1}H NMR (400 MHz, $CDCl_3$) spectrum of {[(IMes)Au]$_3$(μ_3-S)}BF_4.

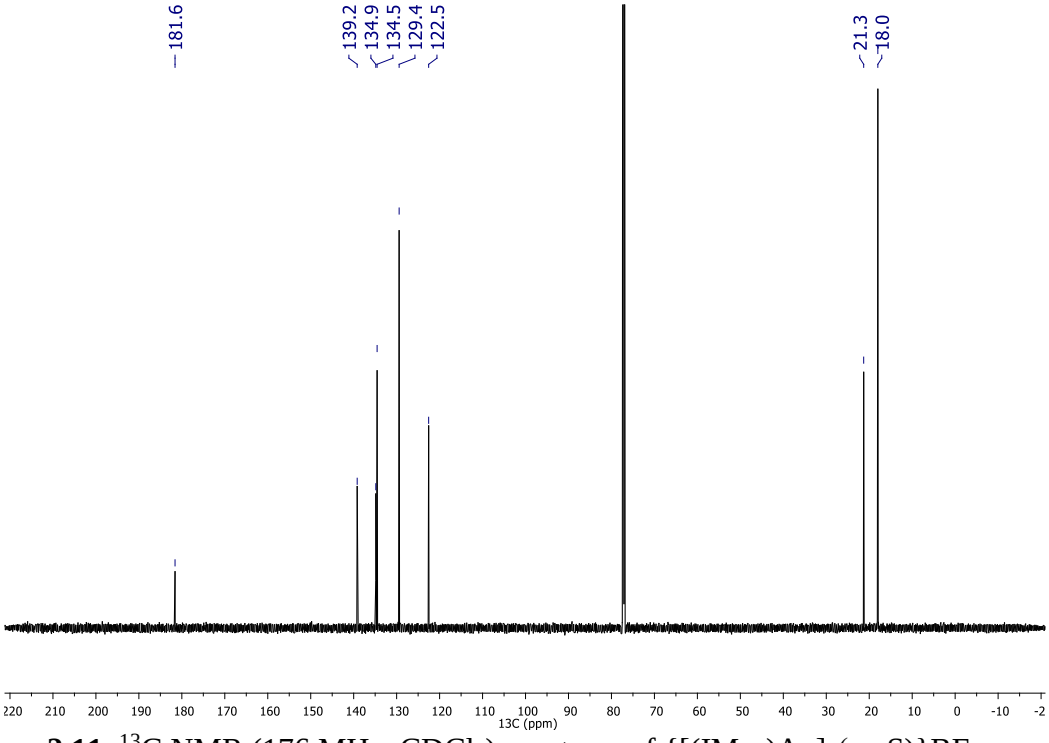

Figure 2.11. ^{13}C NMR (176 MHz, $CDCl_3$) spectrum of {[(IMes)Au]$_3$(μ_3-S)}BF_4.

2.4.3 X-ray Diffraction Data

X-ray diffraction analyses were performed by Dr. John Bacsa, Director of the X-ray Crystallography Lab at Emory University. The crystallographic descriptions below are reproduced with minor adaptations from reports composed by Dr. Bacsa.

2.4.3.1 {[(ICy)Au]$_3$(μ$_3$-S)}OTs

Experimental. Single colorless prism-shaped crystals of {[(ICy)Au]$_3$(μ$_3$-S)}OTs were recrystallized from a mixture of CH_2Cl_2 and hexane by vapor diffusion. A suitable crystal 0.30×0.20×0.10 mm^3 was selected and mounted on a Bruker D8 diffractometer with APEX2 detector diffractometer. The crystal was cooled to T = 100(2) K during data collection. The structure was solved with the ShelXT[20] structure solution program using the Intrinsic Phasing solution method and by using Olex2[21] as the graphical interface. The model was refined with version 2017/1 of ShelXL[22] using Least Squares minimization. **Crystal Data.** $C_{45}H_{72}Au_3N_6S$, M_r = 1320.04, trigonal, $P3_121$ (No. 152), a = 17.5658(5) Å, b = 17.5658(5) Å, c = 32.0726(8) Å, $\alpha = \beta = 90^\circ$, $\gamma = 120^\circ$, V = 8570.4(5) Å^3, T = 100(2) K, Z = 6, Z' = 1, μ(MoK$_\alpha$) = 7.751, 51931 reflections measured, 10427 unique (R_{int} = 0.0699) which were used in all calculations. The final wR_2 was 0.1618 (all data) and R_1 was 0.0640 (I > 2σ(I)).

2.4.3.2 {[(IMes)Au]$_3$(μ$_3$-S)}Cl

Experimental. Single crystals of {[(IMes)Au]$_3$(μ$_3$-S)}Cl were obtained by recrystallization from a mixture of CH_2Cl_2 and hexane by vapor diffusion. A suitable crystal 0.583×0.425×0.333 mm^3 was selected and mounted on a loop with paratone oil on a Bruker APEX-II CCD diffractometer. The crystal was cooled to T= 100(2) K during data collection. Using Olex2,[21] the structure was solved with the XT[20] structure solution

program using Direct Methods and refined with the XL[23] refinement package using Least Squares minimization.

Crystal Data. $C_{65}H_{73.5}Au_3Cl_{1.6}N_7S$, M =1632.57, monoclinic, C2/c (no. 15), a = 14.5178(14) Å, b = 25.154(3) Å, c = 35.496(4) Å, β = 90.020(2)°, α = γ = 90°, V = 12963(2) Å^3, Z = 8, T = 100(2) K, μ(MoKα) = 6.915 mm^{-1}, 102036 reflections measured (3.238° ≤ 2Θ ≤ 62.332°), 20734 unique (R_{int} = 0.0489, R_{sigma} = 0.0354) which were used in all calculations. The final wR_2 was 0.1065 (all data) and R_1 was 0.0441 (I > 2σ(I)).

2.5 References

1. Gimeno, M. C.; Laguna, A., *Chem. Soc. Rev.* **2008,** *37*, 1952-1966.
2. Kowala, C.; Swan, J., *Aust. J. Chem.* **1966,** *19*, 547-554.
3. Angermaier, K.; Schmidbaur, H., *Chem. Ber.* **1994,** *127*, 2387-2391.
4. Wilton-Ely, J. D.; Mitzel, N. W.; Hofreiter, S.; Schmidbaur, H., *Z. Naturforsch. B* **2001,** *56*, 1257-1263.
5. Canales, F.; Gimeno, M. C.; Jones, P. G.; Laguna, A., *Angew. Chem. Int. Ed.* **1994,** *33*, 769-770.
6. Canales, F.; Gimeno, C.; Laguna, A.; Villacampa, M. D., *Inorg. Chim. Acta* **1996,** *244*, 95-103.
7. Canales, F.; Gimeno, M. C.; Laguna, A.; Jones, P. G., *Organometallics* **1996,** *15*, 3412-3415.
8. Gimeno, M. C.; Jones, P. G.; Laguna, A.; Laguna, M.; Terroba, R., *Inorg. Chem.* **1994,** *33*, 3932-3938.
9. Canales, F.; Gimeno, M. C.; Laguna, A.; Jones, P. G., *J. Am. Chem. Soc.* **1996,** *118*, 4839-4845.
10. Robilotto, T. J.; Bacsa, J.; Gray, T. G.; Sadighi, J. P., *Angew. Chem. Int. Ed.* **2012,** *51*, 12077-12080.
11. Polgar, A. M.; Weigend, F.; Zhang, A.; Stillman, M. J.; Corrigan, J. F., *J. Am. Chem. Soc.* **2017,** *139*, 14045-14048.

12. Zhai, J.; Hopkins, M. D.; Hillhouse, G. L., *Organometallics* **2015,** *34*, 4637-4640.

13. Ramamoorthy, V.; Wu, Z.; Yi, Y.; Sharp, P. R., *J. Am. Chem. Soc.* **1992,** *114*, 1526-1527.

14. Schmidbaur, H.; Schier, A., *Chem. Soc. Rev.* **2008,** *37*, 1931-1951.

15. Echavarren, A. M., *Nat. Chem.* **2009,** *1*, 431-433.

16. Marchione, D.; Belpassi, L.; Bistoni, G.; Macchioni, A.; Tarantelli, F.; Zuccaccia, D., *Organometallics* **2014,** *33*, 4200-4208.

17. Bantreil, X.; Nolan, S. P., *Nat. Protoc.* **2011,** *6*, 69-77.

18. Collado, A.; Gomez-Suarez, A.; Martin, A. R.; Slawin, A. M.; Nolan, S. P., *Chem. Commun.* **2013,** *49*, 5541-5543.

19. Fulmer, G. R.; Miller, A. J. M.; Sherden, N. H.; Gottlieb, H. E.; Nudelman, A.; Stoltz, B. M.; Bercaw, J. E.; Goldberg, K. I., *Organometallics* **2010,** *29*, 2176-2179.

20. Sheldrick, G., *Acta Crystallogr. A* **2015,** *71*, 3-8.

21. Dolomanov, O. V.; Bourhis, L. J.; Gildea, R. J.; Howard, J. A. K.; Puschmann, H., *J. Appl. Crystallogr.* **2009,** *42*, 339-341.

22. Sheldrick, G., *Acta Crystallogr. C* **2015,** *71*, 3-8.

23. Sheldrick, G., *Acta Crystallogr. A* **2008,** *64*, 112-122.

CHAPTER 3. TERMINAL AND BRIDGING HYDROSULFIDE GOLD(I) COMPLEXES

3.1 Background

Thiol containing molecules have a large range of uses and studies in biochemistry, nanoparticles, surface chemistry. They are important for their function in protein chemistry for disulfide bond formation and cellular functions.[1-2] For medicinal purposes, gold thiolates of the form LAu(SR) have been used to treat rheumatoid arthritis.[3] From an inorganic perspective, interactions between gold and sulfur have been investigated at the nanoscale, primarily in the use of thiols to cap gold nanoparticles and the formation of self-assembled monolayers (SAM) of gold thiols and thiolates.[4-6]

Despite the number of examples of hydrosulfide metal complexes[7] and gold thiolate complexes,[8-12] there are only a few examples of hydrosulfide gold complexes. Grunwald synthesized an anionic gold(I) hydrosulfide complex, Q[(C_6F_5)Au(SH)] [Q = NEt_4 = tetra-ethylammonium, NBu_4 = tetrabutylammonium, PNP = bis(triphenylphosphoranylidene) ammonium], PNP[(2-$(NO_2)C_6H_4$)Au(SH)] and PNP[(2,4,6-$(NO_2)_3C_6H_2$)Au(SH)] by the addition of H_2S to Q[RAuCl].[13] With further addition of H_2S in a mixture of diethylamine and dichloromethane to Q[RAuSH], an anionic trigold sulfide complex, $Q_2[(RAu)_3(\mu_3\text{-}S)]$ (R = C_6F_5 or 2,4,6-$(NO_2)_3C_6H_2$) was synthesized. The sulfide-bridged complex, $Q_2[(RAu)_2(\mu\text{-}S)]$, could not be isolated, however, it was assumed to have formed during the decomposition of the gold(I) hydrosulfide complex to the trigold sulfide complex due to the smell of H_2S. Gimeno synthesized the first gold(III) hydrosulfide complex, $(NBu_4)[(C_6F_5)_3Au(SH)]$, by treating $(NBu_4)[(C_6F_5)_3AuCl]$ with NaSH.[14] A hydrosulfide-

bridged digold complex was synthesized from the (hydrosulfido)gold(III) complex with the addition of $(C_6F_5)_3Au(OEt_2)$. The hydrogen on the bridging SH could be replaced by either a $(Ph_3P)Au$ or $(Ph_3P)Ag$ forming a trigold sulfide complex containing both Au(III) and Au(I), $Q\{[(C_6F_5)_3Au]_2[(Ph_3P)Au](\mu_3\text{-}S)\}$, and a mixed metal trinuclear sulfide complex, $Q\{[(C_6F_5)_3Au]_2[(Ph_3P)Ag](\mu_3\text{-}S)\}$. There has not been an example of a cationic hydrosulfide gold complex.

This chapter describes the synthesis of the gold(I) hydrosulfide and cationic hydrosulfide-bridged complexes (IPr)AuSH and $\{[(IPr)Au]_2(\mu\text{-}SH)\}OTf$ (IPr = 1,3-bis(2,6-isopropyl phenyl)imidazol-2-ylidene) under ambient conditions. These complexes were air- and moisture-stable. Structural data of these complexes show a linear geometry about the gold for (IPr)AuSH and near-linear gold(I) centers bridged by a bent hydrosulfide in $\{[(IPr)Au]_2(\mu\text{-}SH)\}^+$. The sulfur-bound hydrogens could not be refined; however, proton signals at δ −1.44 ppm for (IPr)AuSH and δ 0.03 ppm for $\{[(IPr)Au]_2(\mu\text{-}SH)\}OTf$ were detected.

3.2 Results and Discussion

3.2.1 Synthesis of (IPr)AuSH

(IPr)AuSH was prepared by mixing (IPr)AuCl with excess sodium hydrosulfide hydrate in ethanol (200 proof) (Scheme 3.1). The reaction of (IPr)AuCl with excess sodium sulfide hydrate also resulted in the formation of (IPr)AuSH; however, these conditions resulted in some formation of $\{[(IPr)Au]_3(\mu_3\text{-}S)\}^+$ as well. Analysis by ^1H NMR shows a single set of IPr signals similar to chemical shifts corresponding to resonances for (IPr)AuCl and a resonance at δ −1.61 ppm. This chemical shift is comparable to those of

anionic organogold hydrosulfides, Q[(C_6F_5)Au(SH)], which give SH signals between δ −1.09 to −1.30 ppm in $CDCl_3$.[13]

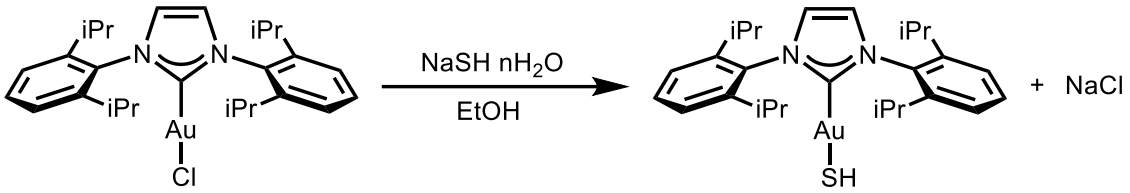

Scheme 3.1. Synthesis of (IPr)AuSH.

3.2.2 X-ray Crystal Structure of (IPr)AuSH

Layering pentane on top of a dichloromethane solution of (IPr)AuSH afforded clear colorless crystals suitable for single crystal X-ray diffraction (Figure 3.1). The carbene-gold-thiol was a linear molecule with a C–Au–S angle of 180°. The Au–S bond distance was shorter than those seen in the IMes or ICy-supported trigold sulfide complexes at 2.2827(8) Å. The Au–C_{NHC} bond distance was similar to those in other NHC gold complexes. The hydrogen on the hydrosulfide could not be refined.

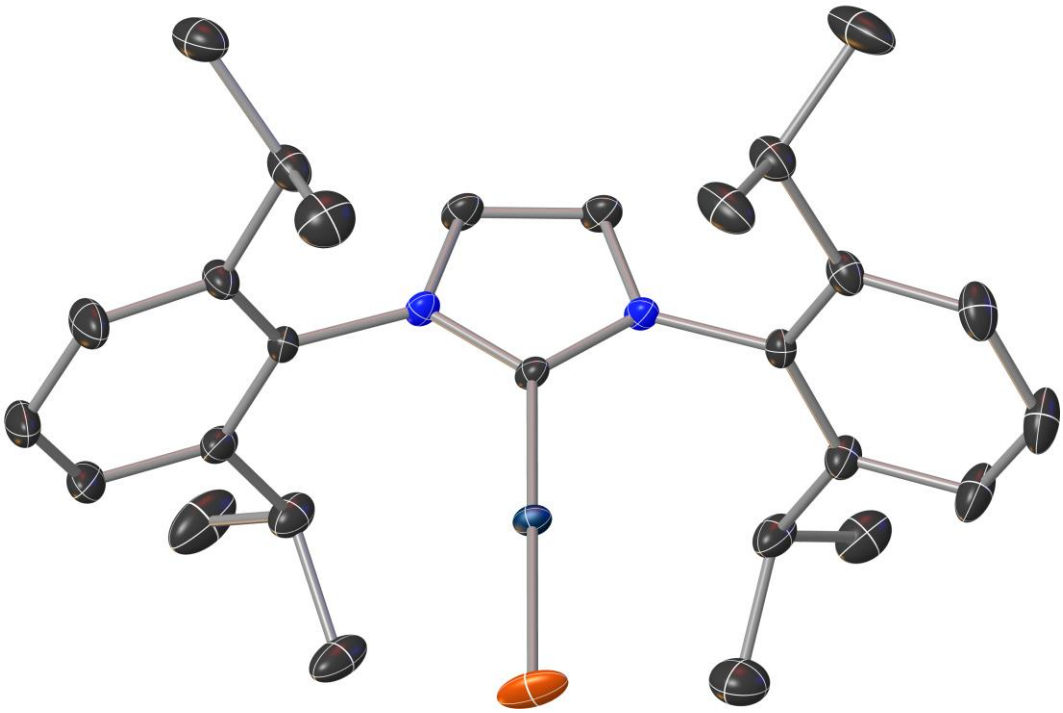

Figure 3.1. Solid state structure of (IPr)AuSH. Hydrogens omitted for clarity. Selected interatomic distances (Å) and angles (°): Au(1)−S(1) 2.2827(8), Au(1)−C(1) 1.991(3); C(1)−Au(1)−S(1) 180.0(1).

3.2.3 Reactivity of (IPr)AuSH

(IPr)AuSH was found to be air- and moisture-stable. Deprotonation of the SH was observed in ^{1}H NMR with potassium tert-butoxide (KO^{t}Bu) in THF-d_8. The disappearance of the hydrosulfide signal, observed at δ −2.04 ppm in THF-d_8 solution, the growth of the methyl group signal for free *tert*-butanol, and the appearance of a new set of IPr resonances was observed.

3.2.4 Synthesis of {[(IPr)Au]$_2$(μ-SH)}OTf

The reaction between (IPr)AuSH and (IPr)AuOTf in dichloromethane yielded the hydrosulfide-bridged cation, {[(IPr)Au]$_2$(μ-SH)}$^{+}$, as its triflate salt (Scheme 3.2). The ^{1}H NMR spectrum of the product complex in $CDCl_3$ shows a single set of IPr resonances as well as the bridging hydrosulfide signal at δ 0.03 ppm. The compound is stable under air,

and in the presence of moisture. The (IPr)AuOTf precursor was stored in the glovebox, but can be handled briefly under air without significant decomposition.

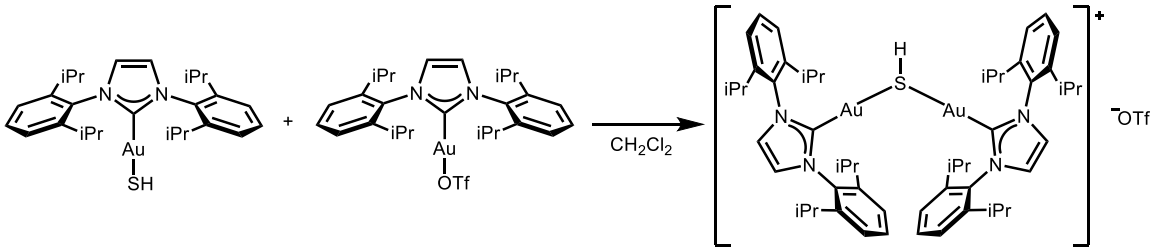

Scheme 3.2. Synthesis of {[(IPr)Au]$_2$(μ-SH)}OTf.

3.2.5 X-ray Crystal Structure of {[(IPr)Au]$_2$(μ-SH)}OTf

Layering pentane on top of a dichloromethane solution of {[(IPr)Au]$_2$(μ-SH)}OTf afforded clear colorless crystals suitable for single-crystal X-ray diffraction (Figure 3.2). The complex crystallizes in the space group, P2$_1$/c; the solvent molecule, dichloromethane, and triflate anion are located outside of the coordination sphere. The Au−S bond distances of 2.2966(6) and 2.3047(6) Å are similar to those of trigold sulfide complexes and of (IPr)AuSH, at around 2.3 Å. The Au−C$_{NHC}$ distances of 1.997(2) and 2.004(2) Å are similar to those in other (NHC)gold complexes and the trigold(I) sulfide complexes using ICy or IMes as ligands. The wide Au(1)−S(1)−Au(2) angle of 116.27(3)° and the long Au(1)−Au(2) distance of 3.9078(5) Å suggest no aurophilic interaction between the gold atoms. This Au−S−Au angle and Au−Au distance is comparable with the those seen in the structures of the anionic hydrosulfide-bridged organogold(III) complex[14] as well as the hydroxide-bridged gold(I) complex using IPr as a ligand.[15]

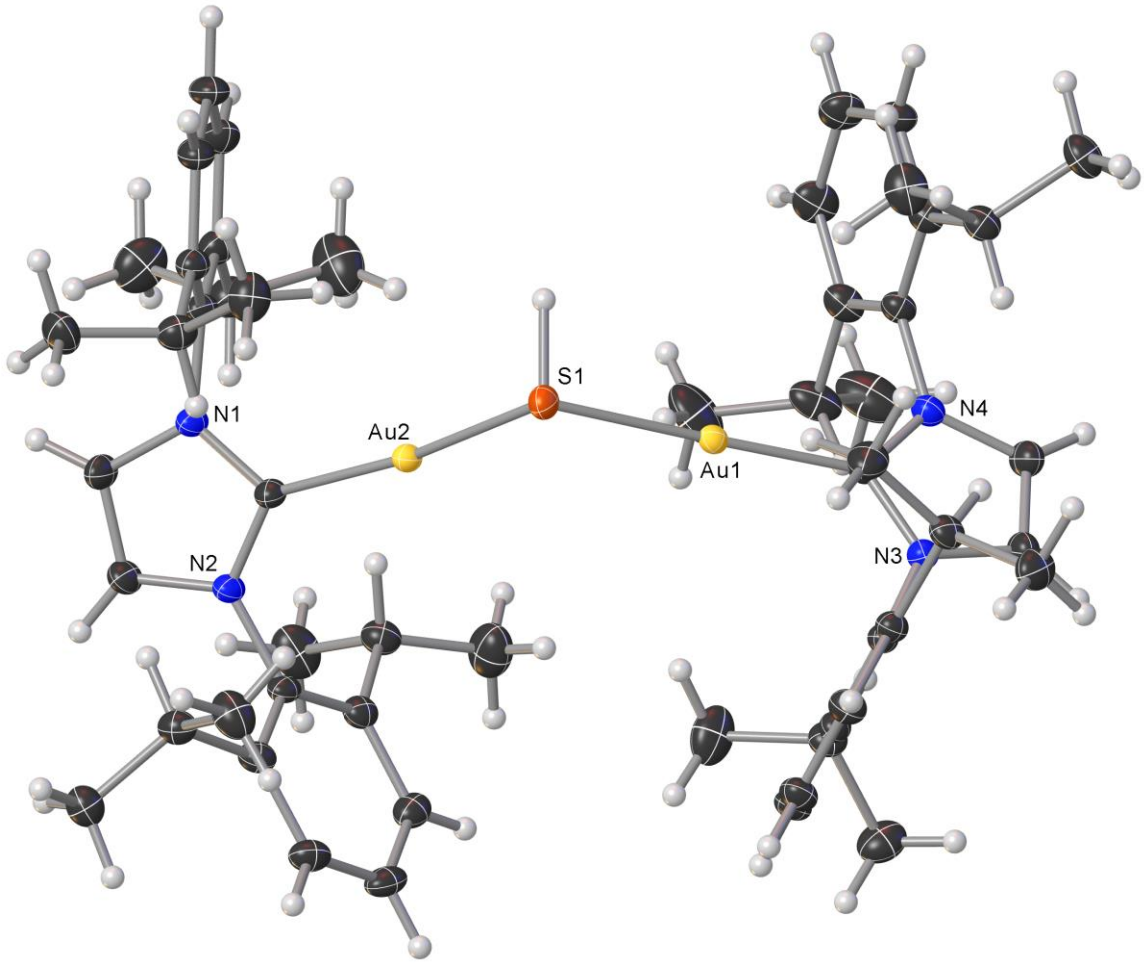

Figure 3.2. Solid state structure of {[(IPr)Au]$_2$(μ-SH)}OTf. Anion omitted for clarity. Selected interatomic distances (Å) and angles (°): Au(1)−S(1), 2.2966(6); Au(2)−S(1), 2.3047(6); Au(1)−C(28), 1.997(2); Au(2)−C(1), 2.004(2); Au(1)−S(1)−Au(2), 116.27(3); C(28)−Au(1)−S(1), 176.28(6); C(1)−Au(1)−S(1), 169.14(7).

3.3 Conclusion

Following the same procedure of the trigold sulfide using ICy and IMes gave a terminal hydrosulfide gold(I) complex using IPr as a supporting ligand. The procedure was refined by using NaSH as the reactant. A cationic bridging-hydrosulfide gold(I) complex has been synthesized from a reaction of the terminal hydrosulfide gold(I) complex and $[LAu]^+$ cation. It was shown that nuclearity of the gold sulfide complex can be controlled using a sterically larger NHC.

3.4 Experimental

3.4.1 General Considerations

Sodium hydrosulfide hydrate (Sigma-Aldrich) were used as received. Dichloromethane (BDH), ethanol (200 proof, KOPTEC), and pentane (EMD) solvents were used as received. IPr•HCl,[16] (IPr)AuCl,[17] and (IPr)AuOTf[18] were synthesized according to literature preparations and characterized by ^{1}H NMR spectroscopy.

^{1}H NMR and ^{13}C NMR spectra were acquired on a Varian Vx 400 MHz spectrometer and a Bruker Avance IIIHD 700 MHz spectrometer. ^{1}H NMR and ^{13}C NMR chemical shifts were referenced with respect to solvent signals relative to tetramethylsilane.[19] Chloroform-*d* (Cambridge Isotope Laboratories) was dried over activated molecular sieves (Alfa Aesar, 4Å).

Elemental analyses were performed by Atlantic Microlab, Inc. in Norcross, Georgia.

3.4.2 Synthetic Procedures

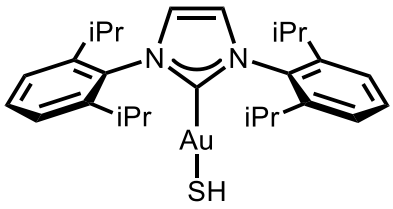

(IPr)AuSH. (IPr)AuCl (0.1400 g, 0.2254 mmol) and excess NaSH • nH$_2$O flakes (0.0847 g, 1.145 mmol, n=3) were stirred in ethanol (5 mL, 200 proof). The solution was briefly sonicated to break up NaSH flakes. The solution was stirred for 6 hours. Ethanol was

removed in vacuo and the white/yellow solid was redissolved in CH_2Cl_2. The redissolved mixture was filtered through Celite, concentrated under vacuum, and the product was precipitated with the addition of pentane. The white solid was filtered and vacuum-dried. The title complex was recrystallized from CH_2Cl_2 layered with pentane to yield needle-like crystals (0.1203 g, 86%). ^{1}H NMR (400MHz, $CDCl_3$): δ (ppm) 7.49 (t, *J* = 7.8 Hz, 2H, C*H*$_{Ar}$), 7.28 (d, *J* = 7.8 Hz, 4H, C*H*$_{Ar}$), 7.14 (s, 2H, NC*H*), 2.59 (sept, *J* = 6.8, 4H, C*H*), 1.34 (d, *J* = 6.9 Hz, 12H, C*H*$_3$), 1.21 (d, *J* = 6.9 Hz, 12H, C*H*$_3$), −1.44 (s, 1H, S*H*). ^{13}C NMR (100MHz, $CDCl_3$): δ (ppm) 187.3 (N*C*Au), 145.8 (*C*$_{Ar}$), 134.3 (*C*$_{Ar}$), 130.6 (*C*$_{Ar}$), 124.3 (*C*$_{Ar}$), 122.9 (N*C*H), 28.9 (*C*H(CH$_3$)$_2$), 24.6 (*C*H$_3$), 24.2 (*C*H$_3$). Anal. calcd for $C_{27}H_{37}AuN_2S$: C, 52.42; H, 6.03; N, 4.53. Found C, 52.58; H 5.98; N, 4.53.

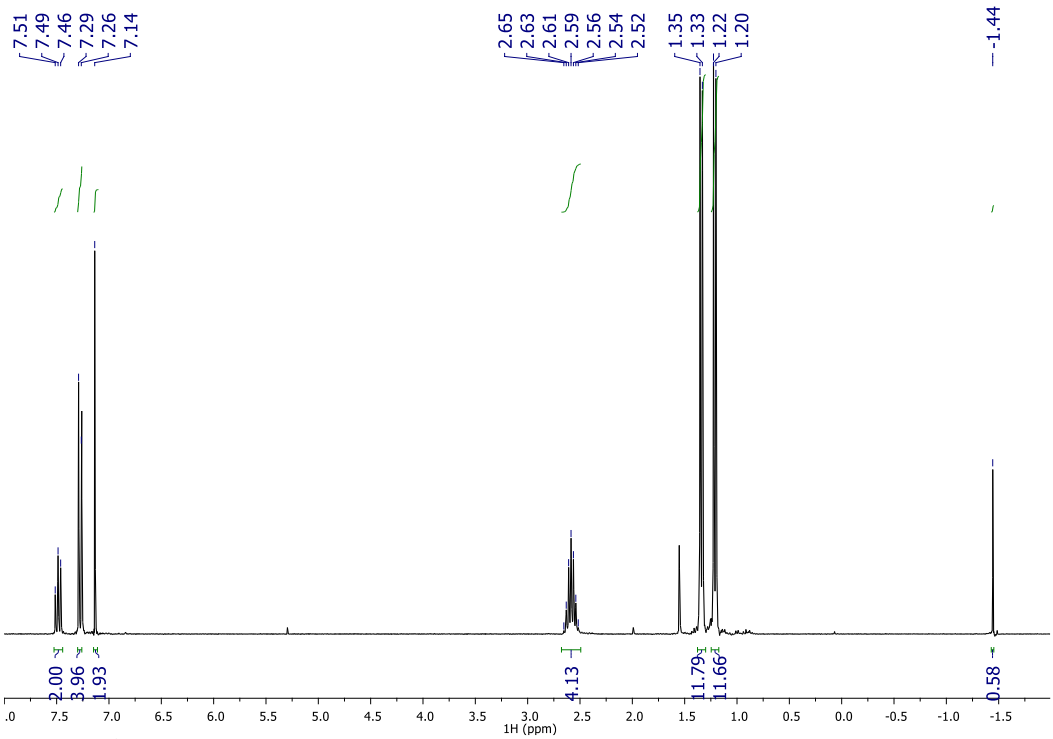

Figure 3.3. ^{1}H NMR (400 MHz, $CDCl_3$) spectrum of (IPr)AuSH. Trace CH_2Cl_2 at δ 5.3 ppm.

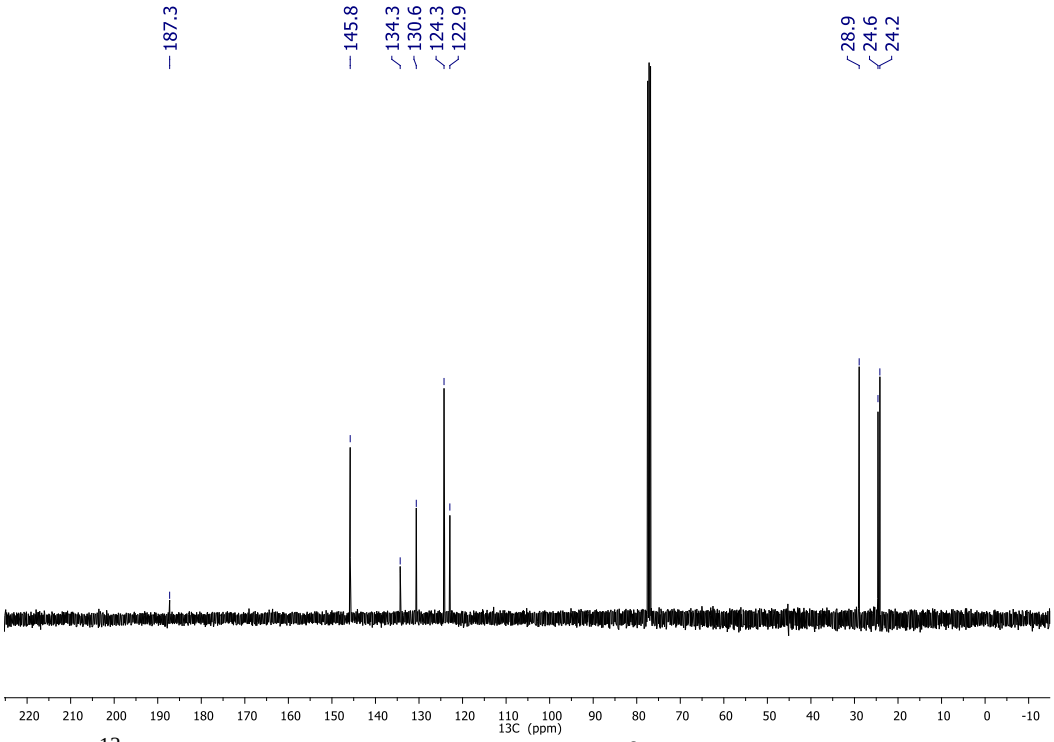

Figure 3.4. ^{13}C NMR (100 MHz, $CDCl_3$) spectrum of (IPr)AuSH.

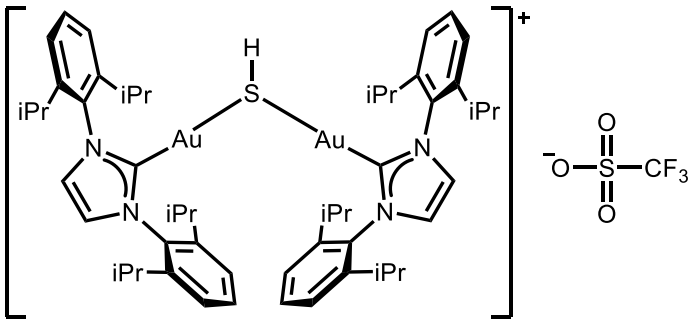

{[(IPr)Au]$_2$(μ-SH)}OTf. (IPr)AuSH (0.050 g, 0.081 mmol) and (IPr)AuOTf (0.064 g, 0.087 mmol) were stirred in CH_2Cl_2 for 1 hour. The solution was filtered through a plug of Celite, concentrated under vacuum, and then crystallized by layering pentane on top of the title complex dissolved in CH_2Cl_2. White crystals were filtered and vacuum dried (0.0904 g, 83% yield). ^1H NMR (400MHz, $CDCl_3$): δ (ppm) 7.49 (t, *J* = 7.8 Hz, 4H, C*H*$_{Ar}$), 7.29 (s, 4H, NC*H*), 7.23 (d, *J* = 7.8 Hz, 8H, C*H*$_{Ar}$), 2.41 (sept, *J* = 6.8 Hz, 8H, C*H*), 1.19 (d, *J* =

6.9 Hz, 24H, C*H*$_3$), 1.09 (d, *J* = 6.9 Hz, 24H, C*H*$_3$), 0.02 (s, 1H, S*H*). ^{13}C NMR (100MHz, $CDCl_3$): δ (ppm) 179.5 (N*C*Au), 145.6 (*C*$_{Ar}$), 133.5 (*C*$_{Ar}$), 130.9 (*C*$_{Ar}$), 124.4 (*C*$_{Ar}$), 124.3 (N*C*H), 28.8 (*C*H(CH$_3$)$_2$), 24.7 (*C*H$_3$), 24.0 (*C*H$_3$). Anal. calcd for $C_{55}H_{73}Au_2F_3N_4O_3S_2$: C, 48.82; H, 5.44; N, 4.14. Found C, 48.96; H, 5.39; N, 4.15.

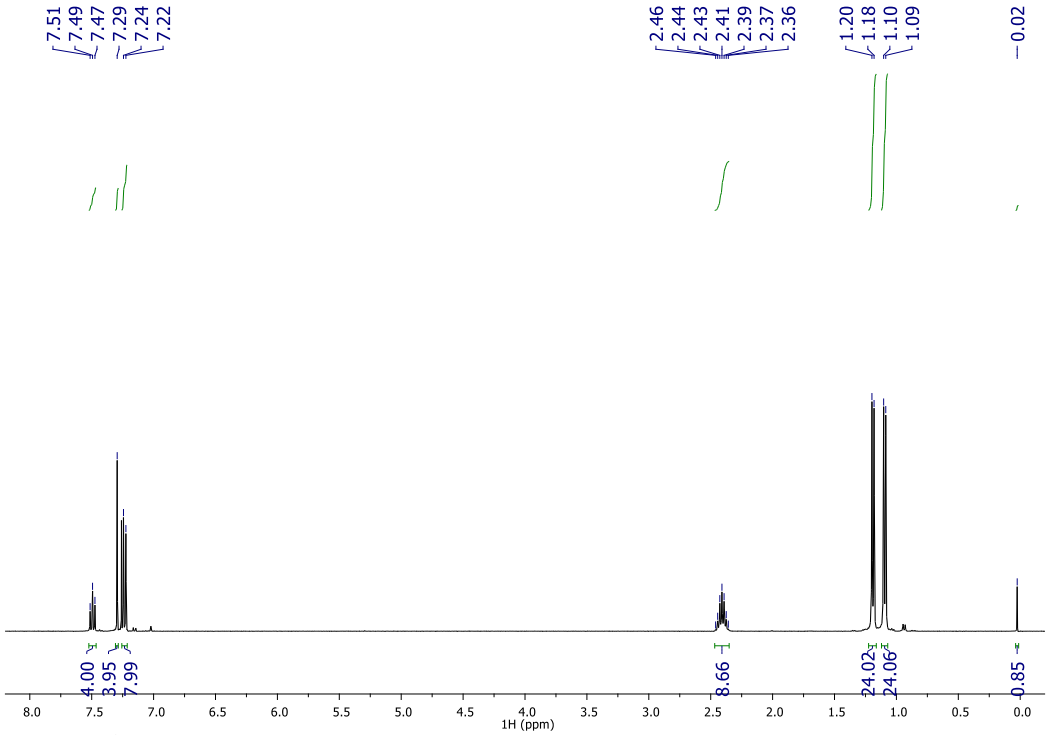

Figure 3.5. ^{1}H NMR (400 MHz, $CDCl_3$) spectrum of {[(IPr)Au]$_2$(μ-SH)}OTf. Trace of {[(IPr)Au]$_3$(μ-S)}$^+$ at δ 7.15, 7.02, and 0.94 ppm.

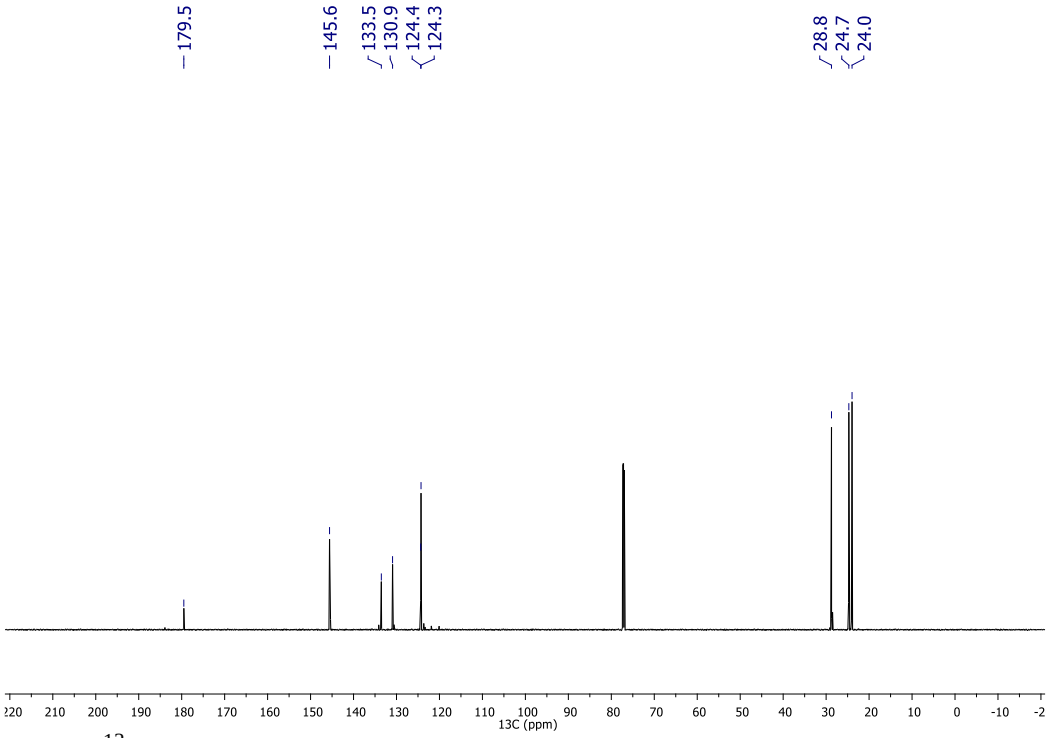

Figure 3.6. ^{13}C NMR (176 MHz, $CDCl_3$) spectrum of {[(IPr)Au]$_2$(μ-SH)}OTf.

3.4.3 X-ray Diffraction Data

X-ray diffraction analyses were performed by Dr. John Bacsa, Director of the X-ray Crystallography Lab at Emory University. The crystallographic descriptions below are reproduced with minor adaptations from reports composed by Dr. Bacsa.

3.4.3.1 (IPr)AuSH

Experimental. Single block-shaped crystals of IPrAuSH were obtained by recrystallization from dissolving the complex in CH_2Cl_2 and layering with pentane. A suitable crystal 0.41×0.27×0.20 mm^3 was selected and mounted on a loop with paratone oil on an SYNERGY diffractometer. The crystal was cooled to T = 100(2) K during data collection. The structure was solved with the ShelXT[20] structure solution program using the Intrinsic Phasing solution method and by using Olex2[21] as the graphical interface. The model was refined with version 2017/1 of ShelXL[22] using Least Squares minimization.

Crystal Data. $C_{27}H_{37}AuN_2S$, M_r = 2470.41, orthorhombic, *Pccn* (No. 56), a = 10.73930(13) Å, b = 12.59559(15) Å, c = 19.6690(2) Å, $\alpha = \beta = \gamma = 90^{\circ}$, V = 2660.58(6) Å^3, T = 100(2) K, Z = 1, Z' = 0.5, μ(MoK$_\alpha$) = 5.623, 83550 reflections measured, 6452 unique (R_{int} = 0.0520) which were used in all calculations. The final wR_2 was 0.0644 (all data) and R_1 was 0.0316 (I > 2σ(I)).

3.4.3.2 {[(IPr)Au]$_2$(μ-SH)}OTf

Experimental. Single colorless prism-shaped crystals of {[(IPr)Au]$_2$(μ-SH)}OTf were obtained by recrystallization from dissolving the complex in CH_2Cl_2 and layering with pentane. A suitable crystal 0.42×0.35×0.20 mm^3 was selected and mounted on a loop with paratone oil on an XtaLAB Synergy, Dualflex, HyPix diffractometer. The crystal was cooled to T = 101(2) K during data collection. The structure was solved with the ShelXT[20] structure solution program using the Intrinsic Phasing solution method and by using Olex2[21] as the graphical interface. The model was refined with version 2017/1 of ShelXL[22] using Least Squares minimization.

Crystal Data. $C_{56}H_{75}Au_2Cl_2F_3N_4O_3S_2$, M_r = 1438.15, monoclinic, $P2_1/c$ (No. 14), a = 18.5763(2) Å, b = 15.96340(10) Å, c = 21.6309(3) Å, β = 109.8930(10)$^{\circ}$, $\alpha = \gamma = 90^{\circ}$, V = 6031.69(12) Å^3, T = 101(2) K, Z = 4, Z' = 1, μ(MoK$_\alpha$) = 5.069 mm^{-1}, 194601 reflections measured, 29225 unique (R_{int} = 0.0563) which were used in all calculations. The final wR_2 was 0.0859 (all data) and R_1 was 0.0344 (I > 2σ(I)).

3.5 References

1. Trivedi, M. V.; Laurence, J. S.; Siahaan, T. J., *Current protein & peptide science* **2009,** *10*, 614-625.

2. Haugaard, N., *Ann. N.Y. Acad. Sci.* **2000,** *899*, 148-158.

3. Mohamed, A. A.; Abdou, H. E.; Chen, J.; Bruce, A. E.; Bruce, M. R. M., *Comments Inorg. Chem.* **2002,** *23*, 321-334.

4. Hakkinen, H., *Nat. Chem.* **2012,** *4*, 443-55.

5. Pensa, E.; Cortés, E.; Corthey, G.; Carro, P.; Vericat, C.; Fonticelli, M. H.; Benítez, G.; Rubert, A. A.; Salvarezza, R. C., *Acc. Chem. Res.* **2012,** *45*, 1183-1192.

6. Vericat, C.; Vela, M. E.; Benitez, G.; Carro, P.; Salvarezza, R. C., *Chem. Soc. Rev.* **2010,** *39*, 1805-1834.

7. Kuwata, S.; Hidai, M., *Coord. Chem. Rev.* **2001,** *213*, 211-305.

8. Sladek, A.; Angermaier, K.; Schmidbaur, H., *Chem. Commun.* **1996**, 1959-1960.

9. Diversi, P.; Cuzzola, A.; Ghiotto, F., *Eur. J. Inorg. Chem.* **2009,** *2009*, 545-553.

10. Battisti, A.; Bellina, O.; Diversi, P.; Losi, S.; Marchetti, F.; Zanello, P., *Eur. J. Inorg. Chem.* **2007,** *2007*, 865-875.

11. Gutiérrez, A.; Bernal, J.; Villacampa, M. D.; Cativiela, C.; Laguna, A.; Gimeno, M. C., *Inorg. Chem.* **2013,** *52*, 6473-6480.

12. Forward, J. M.; Bohmann, D.; Fackler, J. P.; Staples, R. J., *Inorg. Chem.* **1995,** *34*, 6330-6336.

13. Vicente, J.; Chicote, M.-T.; González-Herrero, P.; Grünwald, C.; Jones, P. G., *Organometallics* **1997,** *16*, 3381-3387.

14. Canales, F.; Canales, S.; Crespo, O.; Concepción Gimeno, M.; Jones, P. G.; Laguna, A., *Organometallics* **1998,** *17*, 1617-1621.

15. Ramon, R. S.; Gaillard, S.; Poater, A.; Cavallo, L.; Slawin, A. M.; Nolan, S. P., *Chem. Eur. J.* **2011,** *17*, 1238-1246.

16. Bantreil, X.; Nolan, S. P., *Nat. Protoc.* **2011,** *6*, 69-77.

17. Collado, A.; Gomez-Suarez, A.; Martin, A. R.; Slawin, A. M.; Nolan, S. P., *Chem. Commun.* **2013,** *49*, 5541-5543.

18. Tsui, E. Y.; Muller, P.; Sadighi, J. P., *Angew. Chem. Int. Ed.* **2008,** *47*, 8937-8940.

19. Fulmer, G. R.; Miller, A. J. M.; Sherden, N. H.; Gottlieb, H. E.; Nudelman, A.; Stoltz, B. M.; Bercaw, J. E.; Goldberg, K. I., *Organometallics* **2010,** *29*, 2176-2179.

20. Sheldrick, G., *Acta Crystallogr. A* **2015,** *71*, 3-8.

21. Dolomanov, O. V.; Bourhis, L. J.; Gildea, R. J.; Howard, J. A. K.; Puschmann, H., *J. Appl. Crystallogr.* **2009,** *42*, 339-341.

22. Sheldrick, G., *Acta Crystallogr. C* **2015,** *71*, 3-8.

APPENDIX A. CRYSTALLOGRAPHIC DATA

A1. Crystallographic Data for {[(ICy)Au]$_3$(μ_3-S)}OTs

Table A1.1. Bond Distance in Å for {[(ICy)Au]$_3$(μ_3-S)}OTs

Atom	Atom	Length/Å	Atom	Atom	Length/Å
Au1	Au3	3.1922(12)	N2_2	C4_2	1.469(13)
Au1	S1	2.298(6)	C2_2	C3_2	1.30(2)
Au1	C1_1	2.046(16)	C4_2	C5_2	1.560(19)
Au3	Au2	3.0778(12)	C4_2	C9_2	1.480(18)
Au3	S1	2.294(6)	C5_2	C6_2	1.484(13)
Au3	C1_2	2.009(15)	C6_2	C7_2	1.529(14)
Au2	Au2^1	2.9580(18)	C7_2	C8_2	1.529(14)
Au2	S1	2.309(6)	C8_2	C9_2	1.522(18)
Au2	C1_3	2.051(16)	C10_2	C11_2	1.501(10)
N1_1	C1_1	1.380(17)	C10_2	C15_2	1.501(10)
N1_1	C2_1	1.390(19)	C11_2	C12_2	1.484(13)
N1_1	C10_1	1.470(13)	C12_2	C13_2	1.459(13)
N2_1	C1_1	1.353(17)	C13_2	C14_2	1.459(13)
N2_1	C3_1	1.398(19)	C14_2	C15_2	1.495(17)
N2_1	C4_1	1.469(13)	N1_3	C1_3	1.380(17)
C2_1	C3_1	1.30(2)	N1_3	C2_3	1.389(19)
C4_1	C5_1	1.560(19)	N1_3	C10_3	1.469(13)
C4_1	C9_1	1.481(18)	N2_3	C1_3	1.352(17)
C5_1	C6_1	1.483(13)	N2_3	C3_3	1.398(19)
C6_1	C7_1	1.529(14)	N2_3	C4_3	1.468(13)
C7_1	C8_1	1.529(14)	C2_3	C3_3	1.30(2)
C8_1	C9_1	1.522(18)	C4_3	C5_3	1.560(19)
C10_1	C11_1	1.502(10)	C4_3	C9_3	1.481(18)
C10_1	C15_1	1.502(10)	C5_3	C6_3	1.483(13)
C11_1	C12_1	1.483(13)	C6_3	C7_3	1.529(14)
C12_1	C13_1	1.459(13)	C7_3	C8_3	1.529(14)
C13_1	C14_1	1.459(13)	C8_3	C9_3	1.522(18)
C14_1	C15_1	1.494(16)	C10_3	C11_3	1.501(10)
N1_2	C1_2	1.381(17)	C10_3	C15_3	1.501(10)
N1_2	C2_2	1.389(19)	C11_3	C12_3	1.484(13)
N1_2	C10_2	1.468(13)	C12_3	C13_3	1.459(13)
N2_2	C1_2	1.353(17)	C13_3	C14_3	1.459(14)
N2_2	C3_2	1.398(19)	C14_3	C15_3	1.494(17)

Table A1.2. Bond Angles in ° for {[(ICy)Au]$_3$(μ_3-S)}OTs

Atom	Atom	Atom	Angle/ °
S1	Au1	Au3	45.90(15)
C1_1	Au1	Au3	127.5(5)
C1_1	Au1	S1	171.7(5)
S1	Au3	Au2	48.25(15)
C1_2	Au3	Au2	128.0(5)
C1_2	Au3	S1	175.5(5)
S1	Au2	Au2^1	85.70(15)
C1_3	Au2	Au2^1	95.6(6)
C1_3	Au2	S1	177.8(5)
Au1	S1	Au2	95.1(2)
Au3	S1	Au1	88.1(2)
Au3	S1	Au2	83.9(2)
C1_1	N1_1	C2_1	106.6(12)
C1_1	N1_1	C10_1	124.1(11)
C2_1	N1_1	C10_1	129.1(12)
C1_1	N2_1	C3_1	108.3(12)
C1_1	N2_1	C4_1	120.8(12)
C3_1	N2_1	C4_1	130.2(13)
N1_1	C1_1	Au1	127.6(11)
N2_1	C1_1	Au1	124.8(11)
N2_1	C1_1	N1_1	107.3(12)
C3_1	C2_1	N1_1	109.9(15)
C2_1	C3_1	N2_1	107.6(15)
N2_1	C4_1	C5_1	108.6(11)
N2_1	C4_1	C9_1	112.9(11)
C9_1	C4_1	C5_1	109.2(11)
C6_1	C5_1	C4_1	109.8(12)
C5_1	C6_1	C7_1	110.3(11)
C8_1	C7_1	C6_1	112.4(13)
C9_1	C8_1	C7_1	108.4(12)
C4_1	C9_1	C8_1	112.2(12)
N1_1	C10_1	C11_1	110.1(9)
N1_1	C10_1	C15_1	113.3(10)
C15_1	C10_1	C11_1	111.4(10)
C12_1	C11_1	C10_1	112.1(10)
C13_1	C12_1	C11_1	114.4(11)
C14_1	C13_1	C12_1	111.2(13)
C13_1	C14_1	C15_1	113.6(12)
C14_1	C15_1	C10_1	111.5(11)
C1_2	N1_2	C2_2	106.6(12)
C1_2	N1_2	C10_2	123.5(11)
C2_2	N1_2	C10_2	129.7(12)
C1_2	N2_2	C3_2	108.4(12)
C1_2	N2_2	C4_2	120.3(12)
C3_2	N2_2	C4_2	130.6(13)
N1_2	C1_2	Au3	125.4(11)
N2_2	C1_2	Au3	127.0(11)
N2_2	C1_2	N1_2	107.3(12)
C3_2	C2_2	N1_2	110.0(15)
C2_2	C3_2	N2_2	107.7(15)
N2_2	C4_2	C5_2	108.9(11)
N2_2	C4_2	C9_2	113.0(11)
C9_2	C4_2	C5_2	109.3(11)
C6_2	C5_2	C4_2	109.7(12)
C5_2	C6_2	C7_2	110.3(11)
C8_2	C7_2	C6_2	112.4(13)
C9_2	C8_2	C7_2	108.4(12)
C4_2	C9_2	C8_2	112.0(12)
N1_2	C10_2	C11_2	110.4(9)
N1_2	C10_2	C15_2	113.9(9)
C15_2	C10_2	C11_2	111.4(10)
C12_2	C11_2	C10_2	111.8(10)
C13_2	C12_2	C11_2	114.5(12)
C12_2	C13_2	C14_2	111.5(13)
C13_2	C14_2	C15_2	113.6(12)
C14_2	C15_2	C10_2	111.0(11)
C1_3	N1_3	C2_3	106.6(12)
C1_3	N1_3	C10_3	123.8(11)
C2_3	N1_3	C10_3	129.5(12)
C1_3	N2_3	C3_3	108.5(12)
C1_3	N2_3	C4_3	120.9(12)
C3_3	N2_3	C4_3	130.6(13)
N1_3	C1_3	Au2	120.8(11)
N2_3	C1_3	Au2	132.0(11)
N2_3	C1_3	N1_3	107.3(12)
C3_3	C2_3	N1_3	109.9(15)
C2_3	C3_3	N2_3	107.6(15)
N2_3	C4_3	C5_3	108.7(11)
N2_3	C4_3	C9_3	112.9(11)
C9_3	C4_3	C5_3	109.3(11)
C6_3	C5_3	C4_3	109.9(12)
C5_3	C6_3	C7_3	110.3(11)
C6_3	C7_3	C8_3	112.3(13)
C9_3	C8_3	C7_3	108.3(12)
C4_3	C9_3	C8_3	112.1(12)
N1_3	C10_3	C11_3	110.2(9)
N1_3	C10_3	C15_3	113.5(10)
C15_3	C10_3	C11_3	111.5(10)

Atom	Atom	Atom	Angle/ °
C12_3	C11_3	C10_3	112.0(10)
C13_3	C12_3	C11_3	114.3(11)
C14_3	C13_3	C12_3	111.4(13)
C13_3	C14_3	C15_3	113.7(12)
C14_3	C15_3	C10_3	111.3(11)

A2. Crystallographic Data for {[(IMes)Au]$_3$(μ_3-S)}Cl

Table A2.1. Bond Distance in Å for {[(IMes)Au]$_3$(μ_3-S)}Cl

Atom	Atom	Length/Å
Au1	Au3	3.5216(3)
Au1	Au2	3.5208(4)
Au1	S1	2.3007(11)
Au1	C43	2.011(5)
Au3	Au2	3.5226(4)
Au3	S1	2.3043(12)
Au3	C22	2.018(5)
Au2	S1	2.3032(12)
Au2	C1	2.010(5)
N3	C23	1.430(7)
N3	C22	1.342(7)
N3	C32	1.400(7)
N5	C44	1.435(7)
N5	C43	1.359(7)
N5	C52	1.396(7)
N2	C1	1.340(7)
N2	C13	1.442(7)
N2	C12	1.394(7)
N1	C1	1.370(7)
N1	C2	1.429(8)
N1	C11	1.393(7)
N7	C54	1.440(8)
N7	C43	1.344(7)
N7	C53	1.396(7)
N4	C22	1.359(7)
N4	C34	1.434(8)
N4	C33	1.391(8)
C39	C40	1.506(8)
C39	C34	1.393(8)
C39	C38	1.392(8)
C16	C17	1.401(9)
C16	C15	1.372(10)
C16	C20	1.511(10)
C26	C27	1.369(10)
C26	C25	1.399(9)
C26	C30	1.524(10)
C2	C7	1.408(9)
C2	C3	1.402(8)
C23	C24	1.390(8)
C23	C28	1.409(7)
C13	C18	1.391(8)
C13	C14	1.403(8)
C7	C0AA	1.393(10)
C7	C8	1.485(10)
C3	C4	1.388(8)
C3	C10	1.507(8)
C44	C48	1.406(8)
C44	C6	1.395(8)
C51	C6	1.502(8)
C21	C14	1.515(9)
C24	C25	1.393(9)
C24	C31	1.510(8)
C17	C18	1.394(9)
C11	C12	1.343(10)
C48	C47	1.384(10)
C48	C49	1.507(9)
C6	C45	1.390(8)
C15	C14	1.387(9)
C4	C5	1.392(9)
C27	C28	1.377(9)
C18	C19	1.504(8)
C35	C34	1.398(8)
C35	C36	1.383(10)
C35	C42	1.509(10)
C5	C0AA	1.382(10)
C5	C9	1.504(9)
C60	C59	1.512(9)
C54	C55	1.390(8)
C54	C59	1.398(8)
C46	C45	1.387(9)
C46	C47	1.385(10)
C46	C50	1.501(10)

Atom	Atom	Length/Å	Atom	Atom	Length/Å
C29	C28	1.508(9)	C36	C37	1.398(10)
C38	C37	1.377(9)	C58	C59	1.383(9)
C57	C56	1.391(9)	C32	C33	1.341(10)
C57	C58	1.387(10)	C52	C53	1.354(10)
C57	C61	1.506(10)	C37	C41	1.509(10)
C55	C56	1.395(9)	N1S	C1S	1.1626
C55	C62	1.501(8)	C1S	C2S	1.4526

Table A2.2. Bond Angles in ° for {[(IMes)Au]$_3$(μ_3-S)}Cl

Atom	Atom	Atom	Angle/ °	Atom	Atom	Atom	Angle/ °
Au2	Au1	Au3	60.026(8)	C43	N7	C53	111.3(5)
S1	Au1	Au3	40.15(3)	C53	N7	C54	124.2(5)
S1	Au1	Au2	40.14(3)	C22	N4	C34	126.2(5)
C43	Au1	Au3	146.17(16)	C22	N4	C33	110.5(5)
C43	Au1	Au2	135.85(16)	C33	N4	C34	123.1(5)
C43	Au1	S1	173.15(16)	C34	C39	C40	121.4(5)
Au1	Au3	Au2	59.976(8)	C38	C39	C40	121.0(5)
S1	Au3	Au1	40.08(3)	C38	C39	C34	117.5(5)
S1	Au3	Au2	40.12(3)	C17	C16	C20	120.2(7)
C22	Au3	Au1	135.85(15)	C15	C16	C17	118.8(6)
C22	Au3	Au2	146.12(16)	C15	C16	C20	121.0(7)
C22	Au3	S1	173.19(16)	C27	C26	C25	118.9(6)
Au1	Au2	Au3	59.998(5)	C27	C26	C30	120.9(7)
S1	Au2	Au1	40.09(3)	C25	C26	C30	120.1(7)
S1	Au2	Au3	40.14(3)	N2	C1	Au2	124.2(4)
C1	Au2	Au1	146.28(16)	N2	C1	N1	104.3(4)
C1	Au2	Au3	135.72(15)	N1	C1	Au2	130.9(4)
C1	Au2	S1	173.06(16)	C7	C2	N1	117.3(5)
Au1	S1	Au3	99.77(4)	C3	C2	N1	120.4(5)
Au1	S1	Au2	99.77(4)	C3	C2	C7	122.3(6)
Au2	S1	Au3	99.73(4)	C24	C23	N3	119.1(5)
C22	N3	C23	124.7(5)	C24	C23	C28	121.8(5)
C22	N3	C32	110.7(5)	C28	C23	N3	119.1(5)
C32	N3	C23	124.4(5)	N3	C22	Au3	123.3(4)
C43	N5	C44	126.4(4)	N3	C22	N4	105.2(5)
C43	N5	C52	110.6(5)	N4	C22	Au3	130.9(4)
C52	N5	C44	122.8(5)	C18	C13	N2	119.0(5)
C1	N2	C13	123.6(4)	C18	C13	C14	122.3(5)
C1	N2	C12	111.7(5)	C14	C13	N2	118.7(5)
C12	N2	C13	124.6(5)	C2	C7	C8	122.3(6)
C1	N1	C2	126.0(4)	C0AA	C7	C2	116.8(6)
C1	N1	C11	110.7(5)	C0AA	C7	C8	120.9(6)
C11	N1	C2	123.2(5)	C2	C3	C10	120.7(5)
C43	N7	C54	124.3(5)	C4	C3	C2	117.6(6)

Atom	Atom	Atom	Angle/ °
C4	C3	C10	121.6(5)
C48	C44	N5	117.7(5)
C6	C44	N5	119.9(5)
C6	C44	C48	122.4(6)
C23	C24	C25	117.8(5)
C23	C24	C31	121.1(6)
C25	C24	C31	121.1(6)
C18	C17	C16	122.0(6)
C12	C11	N1	106.7(5)
C44	C48	C49	121.8(6)
C47	C48	C44	117.0(6)
C47	C48	C49	121.2(6)
C44	C6	C51	121.1(5)
C45	C6	C44	117.3(5)
C45	C6	C51	121.6(5)
C16	C15	C14	121.6(6)
C3	C4	C5	122.0(6)
C26	C27	C28	122.3(6)
C13	C18	C17	117.0(5)
C13	C18	C19	121.4(6)
C17	C18	C19	121.5(6)
C34	C35	C42	121.3(6)
C36	C35	C34	117.8(6)
C36	C35	C42	120.9(6)
C4	C5	C9	119.5(7)
C0AA	C5	C4	118.4(6)
C0AA	C5	C9	122.2(7)
C39	C34	N4	119.9(5)
C39	C34	C35	122.2(6)
C35	C34	N4	117.8(5)
C13	C14	C21	121.1(6)
C15	C14	C13	118.1(6)
C15	C14	C21	120.8(6)
C55	C54	N7	118.6(5)
C55	C54	C59	122.6(6)
C59	C54	N7	118.8(5)
N5	C43	Au1	130.7(4)
N7	C43	Au1	123.6(4)
N7	C43	N5	105.1(5)
C45	C46	C50	120.3(7)
C47	C46	C45	118.0(6)
C47	C46	C50	121.7(7)
C23	C28	C29	120.8(6)
C27	C28	C23	117.9(5)
C27	C28	C29	121.3(6)
C37	C38	C39	122.2(6)
C46	C45	C6	122.4(6)
C11	C12	N2	106.5(5)
C56	C57	C61	121.3(7)
C58	C57	C56	118.1(6)
C58	C57	C61	120.6(7)
C54	C55	C56	116.8(5)
C54	C55	C62	121.7(6)
C56	C55	C62	121.5(6)
C35	C36	C37	121.7(5)
C57	C56	C55	122.6(6)
C5	C0AA	C7	122.8(6)
C24	C25	C26	121.3(6)
C48	C47	C46	122.8(6)
C59	C58	C57	121.8(6)
C54	C59	C60	121.2(6)
C58	C59	C60	120.7(6)
C58	C59	C54	118.1(6)
C33	C32	N3	106.7(5)
C32	C33	N4	106.8(6)
C53	C52	N5	106.7(5)
C38	C37	C36	118.5(6)
C38	C37	C41	120.9(7)
C36	C37	C41	120.7(6)
C52	C53	N7	106.3(5)
N1S	C1S	C2S	179.97(7)

A3. Crystallographic Data for (IPr)AuSH

Table A3.1. Bond Distance in Å for (IPr)AuSH

Atom	Atom	Length/Å
Au1	S1	2.2966(6)
Au1	C28	1.997(2)
Au2	S1	2.3047(6)
Au2	C1	2.004(2)
S2	O1	1.429(2)
S2	O2	1.428(3)

Atom	Atom	Length/Å
S2	O3	1.430(3)
S2	C56	1.803(4)
Cl1	C55	1.746(6)
Cl2	C55	1.750(6)
N1	C1	1.351(3)
N1	C16	1.439(3)
N1	C2	1.389(3)
N2	C1	1.349(3)
N2	C4	1.443(3)
N2	C3	1.385(3)
N3	C28	1.351(3)
N3	C43	1.442(3)
N3	C29	1.389(3)
F1	C56	1.346(5)
F2	C56	1.332(5)
N4	C28	1.351(3)
N4	C31	1.446(3)
N4	C30	1.386(3)
C6	C5	1.403(3)
C6	C7	1.376(4)
C5	C4	1.394(3)
C5	C13	1.521(3)
C4	C9	1.397(3)
C3	C2	1.357(3)
C17	C16	1.400(3)
C17	C25	1.515(3)
C17	C18	1.395(3)
C16	C21	1.399(3)
C7	C8	1.391(4)
C14	C13	1.525(4)
C13	C15	1.531(4)
C8	C9	1.399(3)
C9	C10	1.517(3)
C20	C19	1.387(4)
C20	C21	1.389(3)

Atom	Atom	Length/Å
F3	C56	1.315(5)
C19	C18	1.387(4)
C47	C46	1.384(3)
C47	C48	1.393(3)
C46	C45	1.388(3)
C10	C11	1.531(4)
C10	C12	1.523(4)
C45	C44	1.399(3)
C52	C44	1.515(3)
C52	C53	1.526(4)
C52	C54	1.526(4)
C21	C22	1.528(4)
C49	C48	1.518(3)
C49	C50	1.526(4)
C49	C51	1.535(3)
C44	C43	1.402(3)
C31	C32	1.402(3)
C31	C36	1.398(3)
C48	C43	1.400(3)
C25	C26	1.519(4)
C25	C27	1.536(4)
C33	C32	1.395(3)
C33	C34	1.387(4)
C41	C40	1.528(4)
C40	C32	1.516(3)
C40	C42	1.535(4)
C29	C30	1.357(4)
C36	C35	1.398(4)
C36	C37	1.516(4)
C34	C35	1.385(4)
C22	C23	1.541(4)
C22	C24	1.519(4)
C37	C38	1.520(5)
C37	C39	1.535(4)

Table A3.2. Bond Angles in ° for (IPr)AuSH

Atom	Atom	Atom	Angle/°
C28	Au1	S1	176.28(6)
C1	Au2	S1	169.14(7)
Au1	S1	Au2	116.27(3)
O1	S2	O3	115.28(19)
O1	S2	C56	104.92(18)
O2	S2	O1	114.04(19)

Atom	Atom	Atom	Angle/°
O2	S2	O3	114.3(2)
O2	S2	C56	102.50(17)
O3	S2	C56	103.73(19)
C1	N1	C16	125.29(19)
C1	N1	C2	110.94(19)
C2	N1	C16	123.68(19)

Atom	Atom	Atom	Angle/°
C1	N2	C4	124.79(19)
C1	N2	C3	111.02(19)
C3	N2	C4	124.18(18)
C28	N3	C43	123.25(19)
C28	N3	C29	110.55(18)
C29	N3	C43	126.19(19)
N1	C1	Au2	123.68(16)
N2	C1	Au2	130.59(16)
N2	C1	N1	105.1(2)
C28	N4	C31	123.28(19)
C28	N4	C30	110.96(18)
C30	N4	C31	125.58(19)
C7	C6	C5	120.9(2)
C6	C5	C13	120.5(2)
C4	C5	C6	116.6(2)
C4	C5	C13	122.9(2)
C5	C4	N2	117.5(2)
C5	C4	C9	124.3(2)
C9	C4	N2	118.18(19)
C2	C3	N2	106.6(2)
C16	C17	C25	122.3(2)
C18	C17	C16	117.1(2)
C18	C17	C25	120.6(2)
N3	C28	Au1	126.77(15)
N3	C28	N4	105.37(19)
N4	C28	Au1	127.86(15)
C17	C16	N1	119.0(2)
C21	C16	N1	117.6(2)
C21	C16	C17	123.4(2)
C6	C7	C8	120.8(2)
C5	C13	C14	111.8(2)
C5	C13	C15	110.4(2)
C14	C13	C15	112.2(2)
C7	C8	C9	120.8(2)
C4	C9	C8	116.5(2)
C4	C9	C10	121.6(2)
C8	C9	C10	121.8(2)
C3	C2	N1	106.3(2)
C19	C20	C21	120.9(2)
C18	C19	C20	120.6(2)
C46	C47	C48	121.0(2)
C47	C46	C45	120.6(2)
C9	C10	C11	110.2(2)
C9	C10	C12	114.0(2)
C12	C10	C11	109.2(3)

Atom	Atom	Atom	Angle/°
C46	C45	C44	120.7(2)
C44	C52	C53	111.0(2)
C44	C52	C54	111.2(2)
C54	C52	C53	110.8(2)
C16	C21	C22	122.4(2)
C20	C21	C16	117.3(2)
C20	C21	C22	120.3(2)
C48	C49	C50	111.7(2)
C48	C49	C51	110.8(2)
C50	C49	C51	110.5(2)
C45	C44	C52	120.2(2)
C45	C44	C43	117.0(2)
C43	C44	C52	122.8(2)
C32	C31	N4	118.2(2)
C36	C31	N4	118.6(2)
C36	C31	C32	123.1(2)
C47	C48	C49	120.3(2)
C47	C48	C43	117.1(2)
C43	C48	C49	122.6(2)
C17	C25	C26	110.6(2)
C17	C25	C27	112.1(2)
C26	C25	C27	110.9(2)
C44	C43	N3	117.89(19)
C48	C43	N3	118.70(19)
C48	C43	C44	123.4(2)
C34	C33	C32	120.7(2)
C19	C18	C17	120.8(2)
C41	C40	C42	110.9(2)
C32	C40	C41	111.3(2)
C32	C40	C42	110.0(2)
C31	C32	C40	122.3(2)
C33	C32	C31	117.5(2)
C33	C32	C40	120.1(2)
C30	C29	N3	106.8(2)
C31	C36	C37	123.2(2)
C35	C36	C31	117.0(2)
C35	C36	C37	119.7(2)
C35	C34	C33	120.4(2)
C34	C35	C36	121.2(2)
C21	C22	C23	110.3(2)
C24	C22	C21	111.0(2)
C24	C22	C23	110.4(3)
C29	C30	N4	106.4(2)
C36	C37	C38	111.5(3)
C36	C37	C39	110.2(2)

Atom	Atom	Atom	Angle/°	Atom	Atom	Atom	Angle/°
C38	C37	C39	111.3(3)	F3	C56	S2	111.6(3)
F1	C56	S2	112.3(3)	F3	C56	F1	108.4(4)
F2	C56	S2	112.6(3)	F3	C56	F2	106.8(3)
F2	C56	F1	104.7(3)	Cl1	C55	Cl2	113.2(3)

A4. Crystallographic Data for {[(IPr)Au]$_2$(μ-SH)}OTf

Table A4.1. Bond Lengths in Å for {[(IPr)Au]$_2$(μ-SH)}OTf.

Atom	Atom	Length/Å	Atom	Atom	Length/Å
Au1	S1	2.2966(6)	C14	C13	1.525(4)
Au1	C28	1.997(2)	C13	C15	1.531(4)
Au2	S1	2.3047(6)	C8	C9	1.399(3)
Au2	C1	2.004(2)	C9	C10	1.517(3)
S2	O1	1.429(2)	C20	C19	1.387(4)
S2	O2	1.428(3)	C20	C21	1.389(3)
S2	O3	1.430(3)	F3	C56	1.315(5)
S2	C56	1.803(4)	C19	C18	1.387(4)
Cl1	C55	1.746(6)	C47	C46	1.384(3)
Cl2	C55	1.750(6)	C47	C48	1.393(3)
N1	C1	1.351(3)	C46	C45	1.388(3)
N1	C16	1.439(3)	C10	C11	1.531(4)
N1	C2	1.389(3)	C10	C12	1.523(4)
N2	C1	1.349(3)	C45	C44	1.399(3)
N2	C4	1.443(3)	C52	C44	1.515(3)
N2	C3	1.385(3)	C52	C53	1.526(4)
N3	C28	1.351(3)	C52	C54	1.526(4)
N3	C43	1.442(3)	C21	C22	1.528(4)
N3	C29	1.389(3)	C49	C48	1.518(3)
F1	C56	1.346(5)	C49	C50	1.526(4)
F2	C56	1.332(5)	C49	C51	1.535(3)
N4	C28	1.351(3)	C44	C43	1.402(3)
N4	C31	1.446(3)	C31	C32	1.402(3)
N4	C30	1.386(3)	C31	C36	1.398(3)
C6	C5	1.403(3)	C48	C43	1.400(3)
C6	C7	1.376(4)	C25	C26	1.519(4)
C5	C4	1.394(3)	C25	C27	1.536(4)
C5	C13	1.521(3)	C33	C32	1.395(3)
C4	C9	1.397(3)	C33	C34	1.387(4)
C3	C2	1.357(3)	C41	C40	1.528(4)
C17	C16	1.400(3)	C40	C32	1.516(3)
C17	C25	1.515(3)	C40	C42	1.535(4)
C17	C18	1.395(3)	C29	C30	1.357(4)
C16	C21	1.399(3)	C36	C35	1.398(4)
C7	C8	1.391(4)	C36	C37	1.516(4)

Atom	Atom	Length/Å	Atom	Atom	Length/Å
C34	C35	1.385(4)	C37	C38	1.520(5)
C22	C23	1.541(4)	C37	C39	1.535(4)
C22	C24	1.519(4)			

Table A4.2. Bond Angles in ° for {[(IPr)Au]$_2$(μ-SH)}OTf

Atom	Atom	Atom	Angle/°	Atom	Atom	Atom	Angle/°
C28	Au1	S1	176.28(6)	C17	C16	N1	119.0(2)
C1	Au2	S1	169.14(7)	C21	C16	N1	117.6(2)
Au1	S1	Au2	116.27(3)	C21	C16	C17	123.4(2)
O1	S2	O3	115.28(19)	C6	C7	C8	120.8(2)
O1	S2	C56	104.92(18)	C5	C13	C14	111.8(2)
O2	S2	O1	114.04(19)	C5	C13	C15	110.4(2)
O2	S2	O3	114.3(2)	C14	C13	C15	112.2(2)
O2	S2	C56	102.50(17)	C7	C8	C9	120.8(2)
O3	S2	C56	103.73(19)	C4	C9	C8	116.5(2)
C1	N1	C16	125.29(19)	C4	C9	C10	121.6(2)
C1	N1	C2	110.94(19)	C8	C9	C10	121.8(2)
C2	N1	C16	123.68(19)	C3	C2	N1	106.3(2)
C1	N2	C4	124.79(19)	C19	C20	C21	120.9(2)
C1	N2	C3	111.02(19)	C18	C19	C20	120.6(2)
C3	N2	C4	124.18(18)	C46	C47	C48	121.0(2)
C28	N3	C43	123.25(19)	C47	C46	C45	120.6(2)
C28	N3	C29	110.55(18)	C9	C10	C11	110.2(2)
C29	N3	C43	126.19(19)	C9	C10	C12	114.0(2)
N1	C1	Au2	123.68(16)	C12	C10	C11	109.2(3)
N2	C1	Au2	130.59(16)	C46	C45	C44	120.7(2)
N2	C1	N1	105.1(2)	C44	C52	C53	111.0(2)
C28	N4	C31	123.28(19)	C44	C52	C54	111.2(2)
C28	N4	C30	110.96(18)	C54	C52	C53	110.8(2)
C30	N4	C31	125.58(19)	C16	C21	C22	122.4(2)
C7	C6	C5	120.9(2)	C20	C21	C16	117.3(2)
C6	C5	C13	120.5(2)	C20	C21	C22	120.3(2)
C4	C5	C6	116.6(2)	C48	C49	C50	111.7(2)
C4	C5	C13	122.9(2)	C48	C49	C51	110.8(2)
C5	C4	N2	117.5(2)	C50	C49	C51	110.5(2)
C5	C4	C9	124.3(2)	C45	C44	C52	120.2(2)
C9	C4	N2	118.18(19)	C45	C44	C43	117.0(2)
C2	C3	N2	106.6(2)	C43	C44	C52	122.8(2)
C16	C17	C25	122.3(2)	C32	C31	N4	118.2(2)
C18	C17	C16	117.1(2)	C36	C31	N4	118.6(2)
C18	C17	C25	120.6(2)	C36	C31	C32	123.1(2)
N3	C28	Au1	126.77(15)	C47	C48	C49	120.3(2)
N3	C28	N4	105.37(19)	C47	C48	C43	117.1(2)
N4	C28	Au1	127.86(15)	C43	C48	C49	122.6(2)

Atom	Atom	Atom	Angle/°
C17	C25	C26	110.6(2)
C17	C25	C27	112.1(2)
C26	C25	C27	110.9(2)
C44	C43	N3	117.89(19)
C48	C43	N3	118.70(19)
C48	C43	C44	123.4(2)
C34	C33	C32	120.7(2)
C19	C18	C17	120.8(2)
C41	C40	C42	110.9(2)
C32	C40	C41	111.3(2)
C32	C40	C42	110.0(2)
C31	C32	C40	122.3(2)
C33	C32	C31	117.5(2)
C33	C32	C40	120.1(2)
C30	C29	N3	106.8(2)
C31	C36	C37	123.2(2)
C35	C36	C31	117.0(2)

Atom	Atom	Atom	Angle/°
C35	C36	C37	119.7(2)
C35	C34	C33	120.4(2)
C34	C35	C36	121.2(2)
C21	C22	C23	110.3(2)
C24	C22	C21	111.0(2)
C24	C22	C23	110.4(3)
C29	C30	N4	106.4(2)
C36	C37	C38	111.5(3)
C36	C37	C39	110.2(2)
C38	C37	C39	111.3(3)
F1	C56	S2	112.3(3)
F2	C56	S2	112.6(3)
F2	C56	F1	104.7(3)
F3	C56	S2	111.6(3)
F3	C56	F1	108.4(4)
F3	C56	F2	106.8(3)
Cl1	C55	Cl2	113.2(3)